chalcogenide atoms are in the ^1D or ^1S states. While the analogous reaction for Te atoms has not been studied, it is reasonable to expect that similar reactions will occur. We suggest that (trialkylphosphine)tellurides are acting as sources of tellurium which is effectively in an excited atomic state and therefore capable of the observed insertion reactions.

The replacement of 4 equiv of CO by triethylphosphine, which occurs during the formation of **1**, has ample precedent.[4,20] It is known that $(CO)_5MnBr$ reacts with PR_3 (R = alkyl, alkoxide) at 37 °C to give *cis*-$Mn(CO)_3(PR_3)_2Br$ and that this complex isomerizes at 60 °C to the trans isomer. The conditions of formation of **1** are more vigorous, and therefore the ligand replacement proceeds to completion.

In view of the structure of the intermediate **1** the pyrolysis to give MnTe is easily explained. Heating simply removes the labile and volatile two-electron ligands CO and Et_3P. This is analogous to the very well-known decomposition of binary metal carbonyl[21] complexes to give the metal and CO; however, in this case the inorganic nucleus of the complex is bimetallic. It is quite important that this decomposition yields only MnTe. There are other stable phases in the Mn-Te phase diagram, namely Mn, Te, and $MnTe_2$. The fact that none of these are observed to contaminate the solid-state product argues that the stoichiometry of the product is set not only by the stoichiometry of the starting material but also by the nature of the decomposition reaction.

Conclusions

We have discovered a mild method for preparing MnTe using organometallic reagents. The treatment of manganese carbonyl with 2 equiv of (triethylphosphine)telluride in refluxing toluene gives $[(PEt_3)_2(CO)_3MnTe]_2$, which we have isolated and characterized. Subsequent vacuum pyrolysis of this complex yields MnTe as the only nonvolatile product. The structure of **1** and a mechanistic route from starting materials to this intermediate have been discussed.

Supplementary Material Available: Table of thermal parameters (1 page); table of observed and calculated structure factors (29 pages). Ordering information is given on any current masthead page.

(20) (a) Reimann, R. H.; Singleton, E. *J. Organomet. Chem.* **1972**, *44*, C18-20. (b) Reimann, R. H.; Singleton, E. *J. Chem. Soc., Dalton Trans.* **1973**, 841-846.

(21) Wender, I.; Pino, P. *Organic Synthesis via Metal Carbonyls*; Wiley-Interscience: New York, 1968.

Mechanistic Investigation of the ZrMe/PtMe Exchange in $Cp^*ZrMe(\mu\text{-}OCH_2Ph_2P)_2PtMe_2$

Steven M. Baxter, Gregory S. Ferguson, and Peter T. Wolczanski*†

Contribution from the Department of Chemistry, Baker Laboratory, Cornell University, Ithaca, New York 14853. *Received July 20, 1987*

Abstract: The coordinatively unsaturated heterobimetallic, *cis*-$Cp^*Zr(CH_3)(\mu\text{-}OCH_2Ph_2P)_2Pt(CH_3)_2$ (**2a**, $Cp^* = \eta^5\text{-}C_5Me_5$), synthesized via alcoholysis of Cp^*ZrMe_3 by *cis*-$(HOCH_2Ph_2P)_2PtMe_2$ (**1a**), manifested an intermetallic exchange of Me groups through labeling studies. Thermolysis of $Cp^*Zr(CD_3)(\mu\text{-}OCH_2Ph_2P)_2Pt(CH_3)_2$ (**2a-Zr-d_3**) produced $Cp^*Zr(CH_3)(\mu\text{-}OCH_2Ph_2P)_2Pt(CH_3)(CD_3)$ (**2a-Pt-d_3**), as monitored by ^1H NMR. ^{195}Pt NMR crossover experiments utilizing NMR isotope shifts revealed that a scrambling process engendered the concurrent formation of all remaining isotopomers (**2a**, **2a-d_9**, **2a-Zr-d_3/Pt-d_3**, **2a-Pt-d_6**). The rate of crossover, measured by thermolysis of **2a** and **2a-d_9**, was equivalent to the rate of ZrMe/PtMe exchange. From a series of labeling, kinetics, and crossover studies, some involving *cis*-$Cp^*Zr(CH_3)(\mu\text{-}OCH_2CH_2Ph_2P)_2Pt(CH_3)_2$ (**2b**) isotopomers, a mechanism for the overall process is presented. A combination of intramolecular ZrMe/PtMe exchange (k_1) and bimolecular ZrMe/ZrMe scrambling (k_2) reactions comprise the most probable pathway. A kinetic model, derived from specific NMR experiments and checked via simulations, depicts k_1 as the rate-determining step. Activation parameters ($\Delta H^\ddagger = 29.6 \pm 1.0$ kcal/mol, $\Delta S^\ddagger = -5 \pm 3$ eu) may be reconciled by envisioning either five or four (requiring phosphine dissociation) coordinate $(\mu\text{-}CH_3)_2$ transition states/intermediates. Coordinatively saturated $Cp^*Zr(CH_3)_2(\mu\text{-}OCH_2Ph_2P)(CD_3)_2RhCp^*$ (**5-Rh-d_6**) does not undergo Me exchange prior to or during decomposition. Factors contributing to Me transfer, alternative mechanisms, and the relevance of these homogeneous alkyl exchanges to similar heterogeneous processes are discussed.

Heterogeneous catalysts responsible for the making and breaking of C-C and C-O bonds are usually comprised of electron-rich metals deposited on a Lewis acidic metal oxide support.[1,2] The role of the latter cocatalyst ranges from serving as a dispersive medium to one of extensive involvement. In the latter extremes, strong metal support interactions (SMSI) of late metal/early metal oxide catalysts strongly suggest that the components may function in a cooperative fashion.[3] In these instances, the interface between metal oxide and late metal may determine the course of catalytic activity.[4] Late metals and corresponding oxides[5] have exhibited dramatically different reactivity, suggesting that the direct involvement of metal oxides as cocatalysts merits strong consideration.

If early metal oxide supports are reactive, the migration of surface groups across the heterogeneous interface may be critical

† Alfred P. Sloan Foundation Fellow (1987-1989).

(1) (a) Falbe, J. *Chemical Feedstocks from Coal*; John Wiley and Sons: New York, 1981. (b) Dombek, B. D. *Adv. Catal.* **1983**, *32*, 325-416. (c) Bell, A. T. *Catal. Rev.-Sci. Eng.* **1981**, *23*, 203-232. (d) Biloen, P.; Sachtler, W. M. H. *Adv. Catal.* **1981**, *30*, 165-216. (e) Rofer-DePoorter, C. K. *Chem. Rev.* **1981**, *81*, 447-474.

(2) (a) Gault, F. G. *Adv. Catal.* **1981**, *30*, 1-96. (b) Paal, Z. *Ibid.* **1980**, *29*, 273-334. (c) Muetterties, E. L. *Chem. Soc. Rev.* **1982**, *11*, 283-320. (d) *J. Mol. Catal.* **1984**, *25*.

(3) (a) Tauster, S. J. *Acc. Chem. Res.* **1987**, *20*, 389-394. (b) *Strong Metal-Support Interactions*; Baker, R. T. K.; Tauster, S. J.; Dumesic, J. A., Eds.; ACS Symposium Series 298; American Chemical Society: Washington, DC, 1986. (c) *Metal-Support and Metal Additive Effects in Catalysis*; Imelik, B., et al., Eds.; Elsevier: Amsterdam, 1982. (d) Sanchez, M. G.; Gazquez, J. L. *J. Catal.* **1987**, *104*, 120-133, and references therein.

0002-7863/88/1510-4231$01.50/0

in order for the properties of each catalyst component to be effectively utilized. With use of the μ-OCH_2Ph_2P bridging ligand,[6] homogeneous complexes[7,8] which could model such a migration were sought. Linking the O-end of this ligand to an early metal serves to model a $[MO_n]_m$ surface, while the phosphine unit can stabilize late metals in low-valent oxidation states, acceptably modeling a metal (M′) surface.[9]

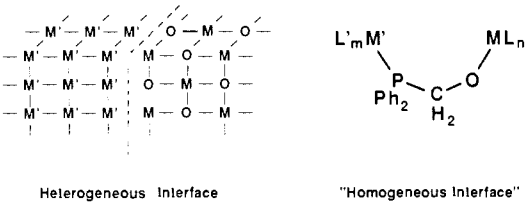

Examples of ligand exchanges[10] between disparate metal centers exist, but, for virtually every case, a strong thermodynamic bias in favor of migration is implicit (e.g., $Cp_2TiMe_2 + (Ph_2MeP)_2PtCl_2 \rightarrow Cp_2TiMeCl + (Ph_2MeP)_2PtCl(Me)$; $\Delta G^\circ \ll 0$).[11] By choosing to investigate thermoneutral migrations (eq 1),[12,13] thermodynamic

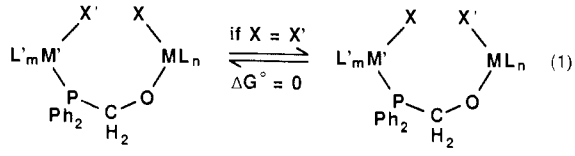

(1)

influences on the rate of transfer may be minimized. This study focuses on the migration of methyl[13-16] between Pt and Zr centers.

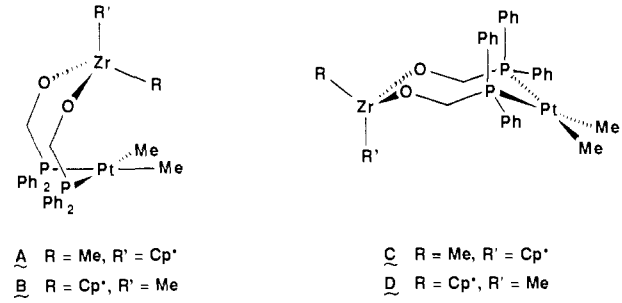

Figure 1. Some possible conformers of $Cp^*ZrMe(\mu\text{-}OCH_2Ph_2P)_2PtMe_2$ (**2a**).

In using a methyl, migration pathways available to groups possessing lone pairs are now obviated; furthermore, the movement of an alkyl[17] is likely to be more relevant to Fischer–Tropsch and reforming processes which make and break C–C bonds. Alkyl migrations may also be likened to surface hydride movements, thereby addressing the phenomenon of hydrogen spillover[18] on heterogeneous catalysts in terms of adsorption on the late metal and migration onto the support. The combination of Zr and Pt is considered representative of typical late (groups 8–10) and early metal oxide composites.[1-4,18]

Results and Discussion

Synthetic Studies. The linking of Zr and Pt moieties via the μ-OCH_2Ph_2P bridge was accomplished via sequential substitution and alcoholysis procedures. When $(COD)PtMe_2$[19] was treated with either $HOCH_2Ph_2P$[20] or $HOCH_2CH_2Ph_2P$[21] the corresponding bis-phosphine derivatives, *cis*-L_2PtMe_2 (L = $HOCH_2Ph_2P$, **1a**; $HOCH_2CH_2Ph_2P$, **1b**),[22-24] were prepared in near quantitative yield (eq 2). Subsequent treatment of **1a** with

$$(COD)PtMe_2 + 2HO(CH_2)_nPh_2P \xrightarrow{-COD} (HO(CH_2)_nPh_2P)_2PtMe_2 \quad (2)$$
$$n = 1,\ \mathbf{1a};\ n = 2,\ \mathbf{1b}$$

(4) (a) Mims, C. A.; McCandlish, L. E. *J. Phys. Chem.* **1987**, *91*, 929–937. (b) Zhang, X.; Biloen, P. *J. Catal.* **1986**, *98*, 468–476. (c) Vannice, M. A.; Sudhaker, C. *J. Phys. Chem.* **1984**, *88*, 2429–2432. (d) Mori, T.; Masuda, H.; Imai, H.; Taniguchi, S.; Miyamoto, A.; Hattori, T.; Murakami, Y. *J. Chem. Soc., Chem. Commun.* **1986**, 1244–1245. (e) Biloen, P.; Helle, J. N.; van den Berg, F. G. A.; Sachtler, W. M. *J. Catal.* **1983**, *81*, 450–458. (f) Dauscher, A.; Garin, F.; Maine, G. *Ibid.* **1987**, *105*, 233–244.

(5) For examples, see: (a) Anton, A. B.; Parmeter, J. E.; Weinberg, W. H. *J. Am. Chem. Soc.* **1986**, *108*, 1823–1833. (b) Anton, A. B.; Avery, N. R.; Toby, B. H.; Weinberg, W. H. *Ibid.* **1986**, *108*, 684–694. (c) Hills, W. M.; Parmeter, J. E.; Weinberg, W. H. *Ibid.* **1987**, *109*, 597–599. (d) Parmeter, J. E.; Schwalke, U.; Weinberg, W. H. *Ibid.* **1987**, *109*, 1876–1877.

(6) (a) Ferguson, G. S.; Wolczanski, P. T. *J. Am. Chem. Soc.* **1986**, *108*, 8293–8295. (b) Ferguson, G. S.; Wolczanski, P. T. *Organometallics* **1985**, *4*, 1601–1605.

(7) For homogeneous organotransition metal modeling of surfaces, see: (a) Bradley, J. S. *Adv. Organomet. Chem.* **1983**, *22*, 1–58. (b) Gladysz, J. A. *Ibid.* **1982**, *20*, 1–38. (c) Herrmann, W. A. *Ibid.* **1982**, *20*, 159–263. (d) Herrmann, W. A. *Angew. Chem., Int. Ed. Engl.* **1982**, *21*, 117–130. (e) Muetterties, E. L.; Stein, J. *Chem. Rev.* **1979**, *79*, 479–490. (f) Muetterties, E. L.; Rhodin, T. N.; Band, E.; Brucker, C. F.; Pretzer, W. R. *Ibid.* **1979**, *79*, 91–137. (g) Tachikawa, M.; Muetterties, E. L. *Prog. Inorg. Chem.* **1981**, *28*, 203–238. (h) Horwitz, C. P.; Shriver, D. F. *J. Am. Chem. Soc.* **1985**, *107*, 8147–8153. (i) Erker, G.; Dorf, U.; Atwood, J. L.; Hunter, W. E. *Ibid.* **1986**, *108*, 2251–2257. (j) Erker, G. *Acc. Chem. Res.* **1984**, *17*, 103–109. (k) Wolczanski, P. T.; Bercaw, J. E. *Ibid.* **1980**, *13*, 121–127.

(8) For early/late bimetallics linked by heterodifunctional bridges, see: Bullock, R. M.; Casey, C. P. *Acc. Chem. Res.* **1987**, *20*, 167–173, and references therein.

(9) The modeling of surfaces through alkoxide and phosphine-ligated transition-metal complexes has been shown to be reasonable. For examples of $(RO)_nM$ models, see: (a) Chisholm, M. H.; Clark, D. L.; Huffman, J. C.; Smith, C. A. *Organometallics* **1987**, *6*, 1280–1291. (b) Chisholm, M. H. *Nouv. J. Chim.* **1987**, *11*, 459–465. For an interesting phosphine-based system, see: Douglas, G.; Manojlović-Muir, L.; Muir, K. W.; Rashidi, M.; Anderson, C. M.; Puddephatt, R. J. *J. Am. Chem. Soc.* **1987**, *109*, 6527–6528.

(10) Garrou, P. E. *Adv. Organomet. Chem.* **1984**, *23*, 95–129.

(11) (a) Puddephatt, R. J.; Stalteri, M. A. *Organometallics* **1983**, *2*, 1400–1405. (b) Pankowski, M.; Samuel, E. *J. Organomet. Chem.* **1981**, *221*, C21–C24.

(12) For a brief mention of an MR/M′R exchange, see: Bryndza, H. E.; Evitt, E. R.; Bergman, R. G. *J. Am. Chem. Soc.* **1980**, *102*, 4948–4951.

(13) For heterodinuclear R/R exchange, see: (a) Park, J. W.; Mackenzie, P. B.; Schaefer, W. P.; Grubbs, R. H. *J. Am. Chem. Soc.* **1986**, *108*, 6402–6404. (b) Mackenzie, P. B.; Ott, K. C.; Grubbs, R. H. *Pure Appl. Chem.* **1984**, *56*, 59–61.

(14) For homodinuclear R/R exchanges, see: (a) Okeya, S.; Meanwell, N. J.; Taylor, B. F.; Isobe, K.; Vazquez de Miguel, A.; Maitlis, P. M. *J. Chem. Soc., Dalton. Trans.* **1984**, 1453–1460. (b) Arnold, D. P.; Bennett, M. A.; McLaughlin, G. M.; Robertson, G. B.; Whittaker, M. J. *J. Chem. Soc., Chem. Commun.* **1983**, 32–34.

(15) For intermolecular MR/MR exchanges, see ref 12 and the following: (a) Ozawa, F.; Ito, T.; Nakamura, Y.; Yamamoto, A. *Bull. Chem. Soc. Jpn.* **1981**, *54*, 1868–1880. (b) Komiya, S.; Albright, T. A.; Hoffmann, R.; Kochi, J. K. *J. Am. Chem. Soc.* **1976**, *98*, 7255–7265. (c) Rice, G. W.; Tobias, R. S. *J. Organomet. Chem.* **1975**, *86*, C37–C40.

(16) For intermolecular MR/M′R (M′ = main group) exchanges, see: (a) Kochi, J. K. *Organometallic Mechanisms and Catalysis*; Academic: New York, 1978. (b) Ozawa, F.; Kurihara, K.; Yamamoto, T.; Yamamoto, A. *J. Organomet. Chem.* **1985**, *279*, 233–243. (c) Oliver, J. P. *Adv. Organomet. Chem.* **1970**, *8*, 167. See, also: Marsella, J. A.; Caulton, K. G. *J. Am. Chem. Soc.* **1982**, *104*, 2361–2365.

(17) An alkyl would result from oligomerization of surface methylenes proposed in the Fischer–Tropsch mechanism: (a) Fischer, F.; Tropsch, H. *Chem. Ber.* **1926**, *59*, 830–836. (b) Brady, R. C., III; Pettit, R. *J. Am. Chem. Soc.* **1981**, *103*, 1287–1289, and references therein. The migration of an R group from M to M′ would occur via alkyl bridges. For examples of the latter, see: (c) Holton, J.; Lappert, M. F.; Pearce, R.; Yarrow, P. I. W. *Chem. Rev.* **1983**, *83*, 135–201. (d) Connelly, N. G.; Forrow, N. J.; Gracey, B. P.; Knox, S. A. R.; Orpen, A. G. *J. Chem. Soc., Chem. Commun.* **1985**, 14–16. (e) Waymouth, R. M.; Santarsiero, B. D.; Coots, R. J.; Bronikowski, M. J.; Grubbs, R. H. *J. Am. Chem. Soc.* **1986**, *108*, 1427–1441. (f) Watson, P. L. *Ibid.* **1983**, *105*, 6491–6493.

(18) (a) Conner, W. C., Jr.; Pajonk, G. M.; Teichner, S. J. *Adv. Catal.* **1986**, *34*, 1–79. (b) Lenz, D. H.; Conner, W. C., Jr. *J. Catal.* **1987**, *104*, 288–298. (c) Bianchi, D.; Lacroix, M.; Pajonk, G. M.; Teichner, S. J. *Ibid.* **1981**, *68*, 411–420. Barbier, J.; Charcosset, H.; de Perriera, G.; Riviere, J. *Appl. Catal.* **1986**, *1*, 71. (d) Maier, W. F. *Nature (London)* **1987**, *329*, 531–534.

(19) Clark, H. C.; Manzer, L. E. *J. Organomet. Chem.* **1973**, *59*, 411–428.

(20) Hellmann, V. H.; Bader, J.; Brikner, H.; Schumacher, O. *Liebigs Ann. Chem.* **1962**, *659*, 49–63.

(21) Bondarenko, N. A.; Matrosov, E. I.; Tsvetkov, E. N.; Kabachnik, M. I. *Izvest. Akad. Nauk SSSR Ser. Khim.* **1980**, *1*, 106–113.

(22) Cheney, A. J.; Mann, B. E.; Shaw, B. L. *J. Chem. Soc., Chem. Commun.* **1971**, 431.

(23) Mather, G. G.; Pidcock, A.; Rapsey, G. J. N. *J. Chem. Soc., Dalton Trans.* **1973**, 2095–2099.

(24) Kennedy, J. D.; McFarlane, R. J.; Puddephatt, R. J.; Thompson, P. H. *J. Chem. Soc., Dalton Trans.* **1976**, 874–879.

Cp^*ZrMe_3[25] resulted in the immediate evolution of CH_4, but monitoring by ^1H NMR revealed that several Cp*-containing species were present. After ~48 h, the desired dinuclear complex, off-white *cis*-$Cp^*ZrMe(\mu\text{-}OCH_2Ph_2P)_2PtMe_2$ (**2a**), may be isolated in 91% yield (eq 3). Apparently, various ligand exchange

$$Cp^*ZrMe_3 + \underset{\mathbf{1a}}{(HOCH_2Ph_2P)_2PtMe_2} \xrightarrow{-2CH_4} \underset{\mathbf{2a}}{\textit{cis}\text{-}Cp^*ZrMe(\mu\text{-}OCH_2Ph_2P)_2PtMe_2} \quad (3)$$

processes may occur during the prolonged post-alcoholysis period, culminating in the highly selective conproportionation to **2a**. The various isotopomers necessary for the ensuing kinetic investigation can be readily obtained via $Cp^*Zr(CD_3)_3$, yielding **2a-Zr-*d*₃** or $(COD)Pt(CD_3)_2$, providing **2a-Pt-*d*₆**. A combination of both deuteriated reagents was used to give **2a-*d*₉**.

The choice of *cis*-$Cp^*ZrMe(\mu\text{-}OCH_2Ph_2P)_2PtMe_2$ (**2a**) in monitoring the Me/Me exchange generically depicted by eq 1 was predicated by inspection of molecular models. As Figure 1 illustrates, four conformations were considered. Two geometries are C-shaped, with either the Zr–Me (A) or the ZrCp* (B) directed toward the top of the Pt square plane. Two crown structures (C and D), with the Cp* and Me groups occupying axial or equatorial positions, presented reasonable alternatives, since this arrangement is common to eight-membered rings.[26] Conformation B suffers from a significant Cp^*/L_2PtMe_2 interaction, thus A is the clear choice of the two C-shaped arrangements. Molecular models of either crown show that the inner phenyl groups from the μ-OCH_2Ph_2P bridges are forced into axial positions. The resulting 1,3-diaxial interaction is greatly reduced upon forming either C-shaped conformer, thus A is most likely the geometry of lowest energy. Interconversions between the various conformers should not be problematic given the floppiness of the ring. In A, the Zr–Me group is posed for either a nucleophilic attack by the Pt d_{z^2} orbital or an electrophilic interaction with an empty Pt p_z, akin to a square-planar substitution.[27] The conformational bias inherent to **2a** was considered to enhance the probability of observing the desired Me migrations.

Both metal centers of **2a** *may* be considered 16e⁻, thus electron deficient.[28] However, in undergoing a Me/Me exchange, electronic unsaturation may not be necessary, since at both metal centers a bond is being broken as another is being made. For comparison, a species with at least one metal electronically saturated was sought. Treatment of $[Cp^*RhCl_2]_2$[29] with 2 equiv of $HOCH_2Ph_2P$ resulted in the formation of $Cp^*RhCl_2(PPh_2CH_2OH)$ (**3**, eq 4) in 97% yield. Alcoholysis of Cp^*ZrMe_3

$$^1/_2[Cp^*RhCl_2]_2 + PPh_2CH_2OH \rightarrow \underset{\mathbf{3}}{Cp^*RhCl_2(PPh_2CH_2OH)} \quad (4)$$

with **3** produced a dinuclear, but during the course of the reaction a thermodynamically predicted Cl/Me exchange also took place, yielding $Cp^*ZrCl_2(\mu\text{-}OCH_2Ph_2P)RhMe_2Cp^*$ (**4**, 78%, eq 5).

$$\mathbf{3} + Cp^*ZrMe_3 \xrightarrow{-CH_4} \underset{\mathbf{4}}{Cp^*ZrCl_2(\mu\text{-}OCH_2Ph_2P)RhMe_2Cp^*} \quad (5)$$

Other exchanges of this type exist,[11] and Cp^*ZrMe_3 has been shown to be a superb alkylating agent, generating $(Me_3P)_2PtMe_2$ from $(Me_3P)_2PtCl_2$ in similar fashion.[30] Subsequent alkylation of **4** with MeMgBr afforded the desired tetraalkyl $Cp^*ZrMe_2(\mu\text{-}OCH_2Ph_2P)RhMe_2Cp^*$ (**5**) in 80% yield (eq 6). Through either $Cp^*Zr(CD_3)_3$ or D_3CMgI the various isotopomers of **5** may be synthesized.

$$\mathbf{4} + 2MeMgBr \xrightarrow{-2MgClBr} \underset{\mathbf{5}}{Cp^*ZrMe_2(\mu\text{-}OCH_2Ph_2P)RhMe_2Cp^*} \quad (6)$$

Kinetic Investigations. The proposed exchange of Me groups (eq 7) between the Zr and Pt centers of **2a** was observed by ^1H NMR by using approach-to-equilibrium kinetics.[31] The equilibrium isotope effect for the apparent **2a-Zr-*d*₃** to **2a-Pt-*d*₃** conversion was considered negligible,[32] thus the equilibrium constant was designated as 2 ($K_{eq} = 2k_1/k_{-1}$), since the Pt center has twice as many Me sites as Zr. The exchange reaction obeyed first-order kinetics, and the first-order rate constants (k_1) ranged from 1.86 (6) × 10^{-7} s^{-1} at 75.6 °C to 3.23 (16) × 10^{-5} s^{-1} at 122.4 °C (Table I). In one instance **2a-Pt-*d*₆** was monitored as an apparent conversion to **2a-Zr-*d*₃/Pt-*d*₃** occurred. The observed rate constant (1.53 (7) × 10^{-6} s^{-1} at 96.4 °C) substantiated the claim of a negligible equilibrium isotope effect, hence K_{eq} for eq 7 remained fixed at 2. After 1.5–2.0 half-lives at 122.4 and 111.8

$$\underset{\mathbf{2a\text{-}Zr\text{-}}d_3}{Cp^*Zr(CD_3)(\mu\text{-}OCH_2Ph_2P)_2Pt(CH_3)_2} \underset{k_{-1}}{\overset{2k_1}{\rightleftharpoons}} \underset{\mathbf{2a\text{-}Pt\text{-}}d_3}{Cp^*Zr(CH_3)(\mu\text{-}OCH_2Ph_2P)Pt(CH_3)(CD_3)} \quad (7)$$

Table I. Rate Constants for the Approach-to-Equilibrium by $Cp^*Zr(CD_3)(\mu\text{-}OCH_2Ph_2P)_2Pt(CH_3)_2$ (**2a-Zr-*d*₃**)

$[\mathbf{2a\text{-}Zr\text{-}}d_3]_0$[a] (M)	k_1 (s^{-1})	T (±0.2 °C)
0.0340	1.3 (1) × 10^{-6}	95.5
0.0560	1.3 (2) × 10^{-6}	96.4
0.0622	1.86 (6) × 10^{-7}	75.6
0.0622	5.56 (1) × 10^{-7}	84.6
0.0622	1.46 (10) × 10^{-6}	96.4
0.0622	1.32 (7) × 10^{-5}	111.8
0.0622	3.23 (16) × 10^{-5}	122.4
0.0680[b]	1.53 (7) × 10^{-6}	96.4
0.0680	1.5 (1) × 10^{-6}	95.5
0.112	1.4 (2) × 10^{-6}	96.4

[a] Benzene-d_6 solutions. [b] Approach-to-equilibrium via **2a-Pt-*d*₆**.

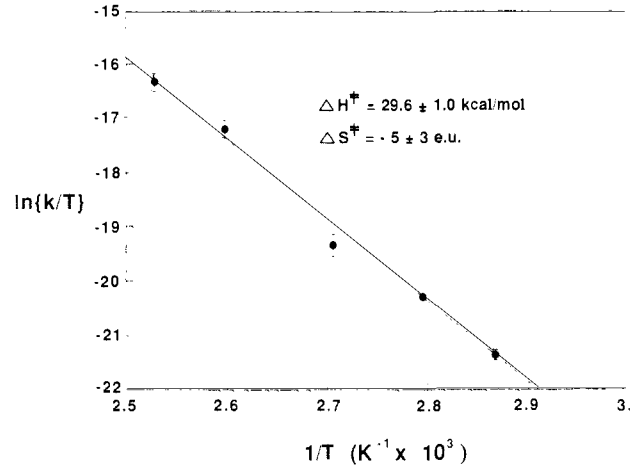

Figure 2. Eyring plot (weighted, linear least squares) for the thermolysis of **2a-Zr-*d*₃**. The weighted, nonlinear least squares gave $\Delta H^\ddagger = 29.3 \pm 1.3$ kcal/mol and $\Delta S^\ddagger = -6 \pm 2$ eu.

(25) Wolczanski, P. T.; Bercaw, J. E. *Organometallics* **1982**, *1*, 793–799.
(26) Eliel, E. L. *Stereochemistry of Carbon Compounds*; McGraw-Hill: New York, 1962.
(27) (a) Basolo, F.; Pearson, R. G. *Mechanisms of Inorganic Reactions*; John Wiley and Sons: New York, 1967. (b) Langford, C. H.; Gray, H. B. *Ligand Substitution Processes*; W. A. Benjamin, Inc.: New York, 1965.
(28) Since the Zr–O–C angles are constrained to deviate from 180° by the bridge, the OR groups are considered neutral 3 e⁻ donors, hence the Zr fragment is 16 e⁻.
(29) Booth, B. L.; Haszeldine, R. N.; Hill, M. *J. Chem. Soc. A* **1969**, 1299–1303.
(30) Ferguson, G. S.; Wolczanski, P. T., unpublished results.
(31) Benson, S. W. *The Foundation of Chemical Kinetics*; McGraw-Hill: New York, 1960.
(32) A secondary equilibrium isotope would be expected to perturb the statistical value ($K = 2$) by an amount well below the experimental error in ^1H NMR integrations. Carpenter, B. K. *Determination of Organic Reaction Mechanisms*; John Wiley and Sons: New York, 1984.

Scheme I

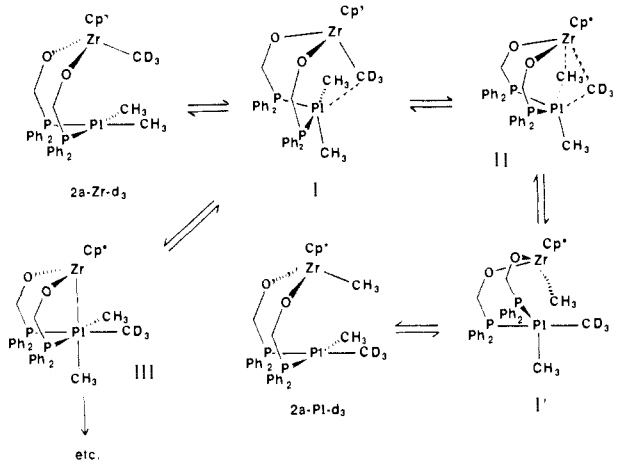

°C, the kinetic plots deviated from linearity due to competitive decomposition of the heterobimetallics. These degradations did not directly affect the exchange rate,[33] but the byproducts interfered with ^{1}H NMR integrations. Lower temperatures proved less problematic; kinetic measurements were limited only by the quality of the integrations (~2.5–3.0 half-lives). Figure 2 manifests the Eyring plot of the rate constants over the 46.8 °C temperature range. The ΔH^* for the process is 29.6 ± 1.0 Kcal/mol, while ΔS^* is −5 ± 3 eu.

Possible Intramolecular ZrMe/PtMe Exchange Pathways. The structure of **2a** was designed to exploit the interaction of the Zr–Me with the top of the Pt(II) square plane. As Scheme I indicates, the exchange of Me groups was viewed as occurring via a pathway similar to a substitution reaction. Intermediate I possesses equatorial P, Pt–CH_3, and μ-CD_3 groups,[17] while the axial positions hold the remaining P and Pt–CH_3. The equivalent of a Berry pseudorotation equilibrates the exchanging methyls via a square pyramidal transition state (II). Since I and I′ are symmetry equivalent, the pathway of I′ to the product is the same as the formation of I. While this pathway is virtually impossible to prove, its features are consistent with the observed data.[34] A substantial amount of bond breaking is implicated by the high ΔH^*, possibly manifesting a greater amount of Zr–Me weakening rather than Pt–Me, since the former is purportedly the stronger bond.[35] The ΔS^* value is less negative than expected but still consistent. A similar pathway involves a limiting structure resulting from addition of the Zr–CD_3 bond[36,37] across the Pt center (III), followed by an elimination of Zr–CH_3.

An alternative and perhaps more attractive view of the exchange (vide infra) is illustrated by Scheme II. As the $ZrCD_3$ enters the coordination sphere of the Pt moiety, one bridging phosphine dissociates. The displacement, not unlike a common square-planar substitution,[27] leads initially to the formation of a new square-planar species containing a μ-CD_3 (IV). Formation of a second bridging methyl leads to an intermediate or transition state that

Scheme II

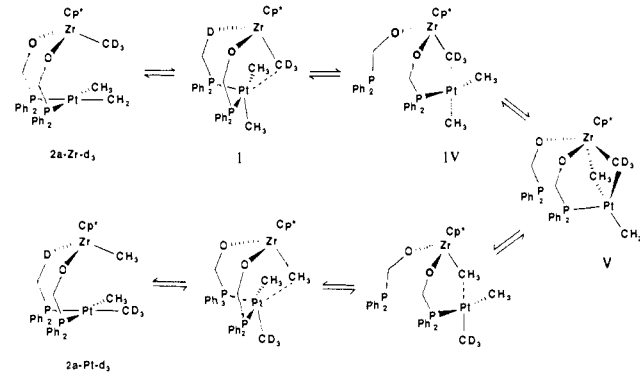

is T_d about Pt (V). Although the latter species possesses asymmetric μ-Me groups,[17] there is little distinction in breaking either bridging methyl, only one of which is productive toward exchange. In effect, a turnstile involving two μ-Me groups and one terminal Pt–Me of the tetrahedral species causes equilibration. An alternative to this assisted displacement process is a straightforward dissociation leading to a three-coordinate Pt center, which can then be trapped by a Zr–CD_3 to form μ-CD_3-containing IV.

Ligand dissociation is known to precede Me redistributions in square planar[10,15,38] and other systems[15] where the vacant coordination site is presumed to actively promote alkyl exchange. The assisted loss of phosphine is tenuously preferred since associative pathways are prevalent for square-planar substitutions[27] and ΔH^* is somewhat low with respect to phosphine dissociation enthalpies.[39] A constrained, yet dissociated transition state/intermediate such as IV is also supported by the small, negative ΔS^*. Attempts to substantiate Scheme II through inhibition studies were uninformative; when PPh_3 was added to **2a-Zr-*d*$_3$**, it decomposed to several unidentifiable products. Furthermore, **2a** degraded when dissolved in polar solvents such as THF, pyridine, acetonitrile, and hot CH_2Cl_2, effectively limiting the experimental medium to hydrocarbons. The unprovable details separating the two similar schemes represent minor problems since the primary objective, observing an intermetallic alkyl transfer, has clearly been realized. However, the distinction between the higher coordinate intermediates of Scheme I and the phosphine-dissociated species of Scheme II may be critical in specifying the overall transformation (vide infra).

Although the Pt/Zr exchange reaction proceeded in a fairly smooth fashion, the corresponding reaction in $Cp^*Zr(CH_3)_2(\mu$-$OCH_2Ph_2P)Rh(CD_3)_2Cp^*$ (**5-Rh-*d*$_6$**) could not be observed prior to or during decomposition (~100 °C, eq 8). Degradation of

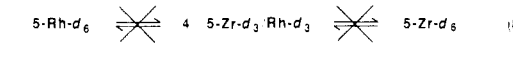

5-Rh-*d*$_6$ presumably follows breakage of the Rh–P link. This result tentatively implies that exchange processes need sites of coordinative unsaturation at both metal centers. Garrou has reviewed a number of ligand redistribution reactions and virtually all appear to be restricted in this same manner.[10] At the very least, existing coordination sites greatly facilitate this class of reactions.

Although the premise for this study, the observation of heterobimetallic alkyl/alkyl exchange, has been experimentally verified, a more detailed investigation of the overall mechanism indicates that the transformation is more complex than originally thought.

Crossover Experiments. The Me/Me swap of **2a-Zr-*d*$_3$** (eq 7) was observed to be first order, indicating the molecularity of reaction prior to or during the rate-determining step. To probe the possibility of a post-rate-determining scrambling process, a crossover experiment was conducted. Fully deuteriated **2a-*d*$_9$** and **2a** were heated at 96.4 °C for 2 days, and *crossover was observed*

(33) The degradation rate, estimated through thermolysis of unlabeled **2a** in the presence of an internal standard, could be used to correct the PtMe/ZrMe exchange rate. Degradation products were subsequently shown to have no effect on the latter reaction rate. At the lower temperatures the degradation was too slow to be observed on the timescale of the exchange.

(34) Similar, nondissociative exchanges have been suggested for bimolecular processes. For example, see: (a) Puddephatt, R. J.; Thompson, P. J. *J. Chem. Soc., Dalton Trans.* **1977**, 1219–1223. (b) Puddephatt, R. J.; Thompson, P. J. *Ibid.* **1975**, 1810–1816.

(35) For experimental and estimated bond strengths of early and late metal alkyls, see: (a) Nolan, S. P.; Hoff, C. D.; Stoutland, P. O.; Newman, L. J.; Buchanan, J. M.; Bergman, R. G.; Yang, G. K.; Peters, K. S. *J. Am. Chem. Soc.* **1987**, *109*, 3143–3145. (b) Bryndza, H. E.; Fong, L. K.; Paciello, R. A.; Tam, W.; Bercaw, J. E. *Ibid.* **1987**, *109*, 1444–1456. (c) Bruno, J. W.; Marks, T. J.; Morss, L. R. *Ibid.* **1983**, *105*, 6824–6832, and references therein.

(36) The addition of Zr–Me to Rh to generate a MeRh–Zr moiety has been verified by X-ray structure determination: Ferguson, G. S.; Wolczanski, P. T.; Párkányi, L.; Zonnevylle, M. C., submitted for publication.

(37) Ling, S. M.; Payne, N. C.; Puddephatt, R. J. *Organometallics* **1985**, *4*, 1546–1550.

(38) Scott, J. D.; Puddephatt, R. J. *Organometallics* **1983**, *2*, 1643–1648.

(39) (a) Nolan, S. P.; de la Vega, R. L.; Hoff, C. D. *Organometallics* **1986**, *5*, 2529–2537. (b) Manzer, L. E.; Tolman, C. A. *J. Am. Chem. Soc.* **1975**, *97*, 1955–1956. (c) Tolman, C. D. *Chem. Rev.* **1977**, *77*, 313–348.

Table II. Relative Equilibrium Concentrations of $Cp^*ZrCH_3(\mu\text{-}OCH_2Ph_2P)_2Pt(CH_3)_2$ (**2a**) Isotopomers

CH_3/CD_3	[Σ 2α's]	[**2a**]	[**2a-Zr-d_3**]	[**2a-Pt-d_3**]	[**2a-Zr-d_3/Pt-d_3**]	[**2a-Pt-d_6**]	[**2a-d_9**]
2	1.00	0.2963	0.1481	0.2963	0.1481	0.0741	0.0371
1	1.00	0.125	0.125	0.250	0.250	0.125	0.125
0.5	1.00	0.0370	0.0741	0.1481	0.2963	0.1481	0.2963

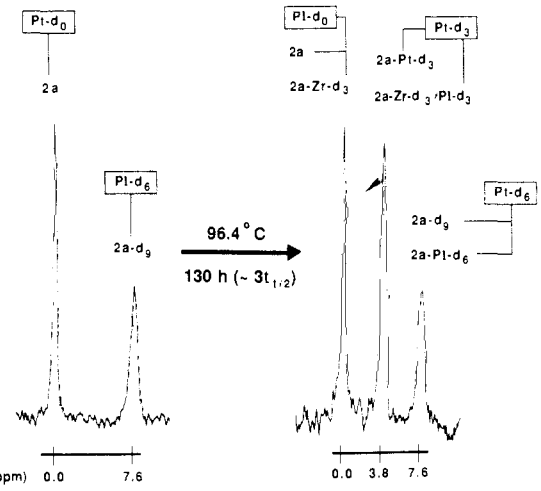

Figure 3. $^{195}Pt\{^1H\}$ NMR monitoring of the **2a** + **2a-d_9** crossover experiment.

via $^{195}Pt\{^1H\}$ NMR.[40] The spectrum of **2a** (and **2a-Zr-d_3**) consists of a triplet at δ −4690 (J_{PtP} = 1830 Hz); these resonances are shifted upfield by ~7.6 ppm when the Pt is coordinated by two CD_3 groups (**2a-Pt-d_6**; **2a-d_9**) due to an NMR isotope effect.[41,42] The crossover was kinetically monitored (1.7 (1) × 10^{-6} s^{-1}) via the growth of a resonance ~3.8 ppm upfield of **2a**, indicative of a Pt center containing one CD_3 (**2a-Zr-d_3/Pt-d_3**; Figure 3). By using **2a-Pt-d_6**, the methyl exchange was simultaneously monitored by ^1H NMR (1.53 (7) × 10^{-6} s^{-1}) and *simplified* $^{195}Pt\{^1H\}$ NMR (1.2 × 10^{-6} s^{-1}, **Pt-d_6** ⇌ **Pt-d_3**) kinetics. Extended thermolysis resulted in the formation of **Pt-d_0** products, indicative of crossover. In conjunction with the latter, **2a-Zr-d_3** was also observed to form **Pt-d_3** and **Pt-d_6** species upon heating. Clearly, the similarities in the ^1H and $^{195}Pt\{^1H\}$ NMR experiments suggest that the first-order process for exchange matches that of the scrambling.

From the crossover studies it can be inferred that at equilibrium, all **2a** isotopomers are present in concentrations depending on the number of CD_3 groups present in the thermolysis precursor(s) (Table II). In addition, the original intermetallic approach to equilibrium in eq 7 is better represented by the conversion of **2a-Zr-d_3** to the distribution in eq 9. In this treatment, $2k'_1/k'_{-1}$

$$[Zr\text{–}CD_3] \underset{k'_{-1}}{\overset{2k'_1}{\rightleftharpoons}} [Pt\text{–}CD_3] \qquad (9)$$

initially: $[Zr\text{–}CD_3]$ = [**2a-Zr-d_3**]

equilibrium:

$[Zr\text{–}CD_3]$ = [**2a-Zr-d_3**] + [**2a-Zr-d_3/Pt-d_3**] + [**2a-d_9**]

$[Pt\text{–}CD_3]$ =

[**2a-Pt-d_3**] + [**2a-Zr-d_3/Pt-d_3**] + 2[**2a-Pt-d_6**] + 2[**2a-d_9**]

refers to the ratio of $Pt\text{–}CD_3$ to $Zr\text{–}CD_3$ groups at equilibrium. Given the initial conditions of this experiment ($[Zr\text{–}CD_3]$ = [**2a-Zr-d_3**], $[Pt\text{–}CD_3] \cong 0$), it is not clear whether the phenomenological rate constant k'_1 is equivalent to the desired rate constant k_1, the direct exchange of Me's between Zr and Pt. The statistical distribution in eq 9 is the same as eq 7; $2k'_1/k'_{-1} = 2$, assuming negligible equilibrium isotope effects. Similar comments pertain to the approach to equilibrium by **2a-Pt-d_6**; the observed rate constants ($2k'_1/k'_{-1}$, eq 10) may not be equivalent to a

$$[Zr\text{–}CH_3] \underset{k'_{-1}}{\overset{2k'_1}{\rightleftharpoons}} [Pt\text{–}CH_3] \qquad (10)$$

initially: $[Zr\text{–}CH_3]$ = [**2a-Pt-d_6**]

equilibrium: $[Zr\text{–}CH_3]$ = [**2a**] + [**2a-Pt-d_3**] + [**2a-Pt-d_6**]

$[Pt\text{–}CH_3]$ =

2[**2a-Zr-d_3**] + [**2a-Zr-d_3/Pt-d_3**] + 2[**2a-Pt-d_3**] + 2[**2a**]

one-step intermetallic exchange ($2k_1/k_{-1}$) generating **2a-Zr-d_3/Pt-d_3**, but the statistics of the process remain unchanged. Questions must also be raised about the meaning of the first-order rate constants obtained from the ^{195}Pt NMR kinetics. As will be shown, in certain cases the true bimetallic exchange rate, k_1, may be extracted from the experimental observables (see Appendix).

Although the course of methyl exchange is underdetermined, two possible origins of crossover may be eliminated. First, assuming the crossover and ZrMe/PtMe exchange rates are the same, no PtMe/PtMe transfers may take place prior to the rate-determining step. If this occurred, the ^{195}Pt NMR experiments would have manifested the exchange at a rate faster than the ZrMe/PtMe transfer. Second, any rational ZrMe/ZrMe exchange would necessarily be bimolecular in origin;[11,43] the Zr centers are unsaturated, and no realistic ligand dissociation pathways are available. Potential exchanges must then be envisioned as occurring through $Zr(\mu\text{-}Me)_2Zr$ bridged[17] transients. In order for a post-rate-determining bimolecular ZrMe/ZrMe swap to account for crossover, it must be of comparable rate to the first-order bimetallic exchange. Since the crossover is concentration independent under conditions where it can be observed, any second-order ZrMe/ZrMe exchange must occur prior to the rate-determining step.

Mechanistic Hypotheses. How the Zr and Pt centers trade methyl groups poses an interesting mechanistic puzzle. The crossover experiments suggest two major possibilities: (1) ZrMe/PtMe exchanges may be intermolecular, provided they are post-rate-determining and (2) fast pre-rate-determining, bimolecular ZrMe/ZrMe or post-rate-determining PtMe/PtMe exchange processes could explain the observed scrambling, if ZrMe/PtMe swaps *only* occur intramolecularly. The first contention is somewhat disturbing, since **2a** was designed to undergo an intramolecular process, yet the latter would also seem unlikely, requiring either rather specific and/or somewhat fast intermolecular alkyl exchanges.

Scheme III shows three possible sequences leading to ZrMe/PtMe exchange. Each manifests *only* one crossover and *only* one intermetallic exchange step, all illustrated by the combination of **2a** + **2a-d_9**. In A, the intermetallic exchange is intermolecular, and phosphine dissociation (to **I-d_0**, akin to **IV** of Scheme II) is rate-determining; this type of exchange *alone* is enough to accommodate the crossover results. Fast pre-rate-determining ZrMe/ZrMe or post-rate-determining ZrMe/ZrMe and PtMe/PtMe processes could also be present, given the similarity in crossover and exchange rates (vide supra). Pathway B exhibits an intramolecular ZrMe/PtMe transfer path via phosphine-dissociated intermediate **I-d_0** where post-rate-determining PtMe/PtMe transfers (**I-d_0** + **2a-d_9** → **I-Pt-d_3** + **2a-Zr-d_3/Pt-d_3**) give rise to crossover. The last route shown, C, implicates fast ZrMe/ZrMe exchange[43] prior to a rate-determining intramo-

(40) Pregosin, P. S. *Coord. Chem. Rev.* **1982**, *44*, 247–291.
(41) Jameson, C. J. *J. Chem. Phys.* **1977**, *66*, 4983–4988.
(42) For other examples of ^{195}Pt isotope shifts, see: (a) Ismail, I. S.; Kerrison, J. S.; Sadler, P. J. *J. Chem. Soc., Chem. Commun.* **1980**, 1175–1176 (Cl, Br). (b) Groning, O.; Drakenberg, T.; Elding, L. I. *Inorg. Chem.* **1982**, *21*, 1820–1824 ($^{16}O/^{18}O$).
(43) (a) Lubben, T. V.; Wolczanski, P. T. *J. Am. Chem. Soc.* **1987**, *109*, 424–435. (b) Jordon, R. *J. Organomet. Chem.* **1985**, *294*, 321–326. (c) Marsella, J. A.; Moloy, K. G.; Caulton, K. G. *Ibid.* **1980**, *201*, 389.

Scheme III

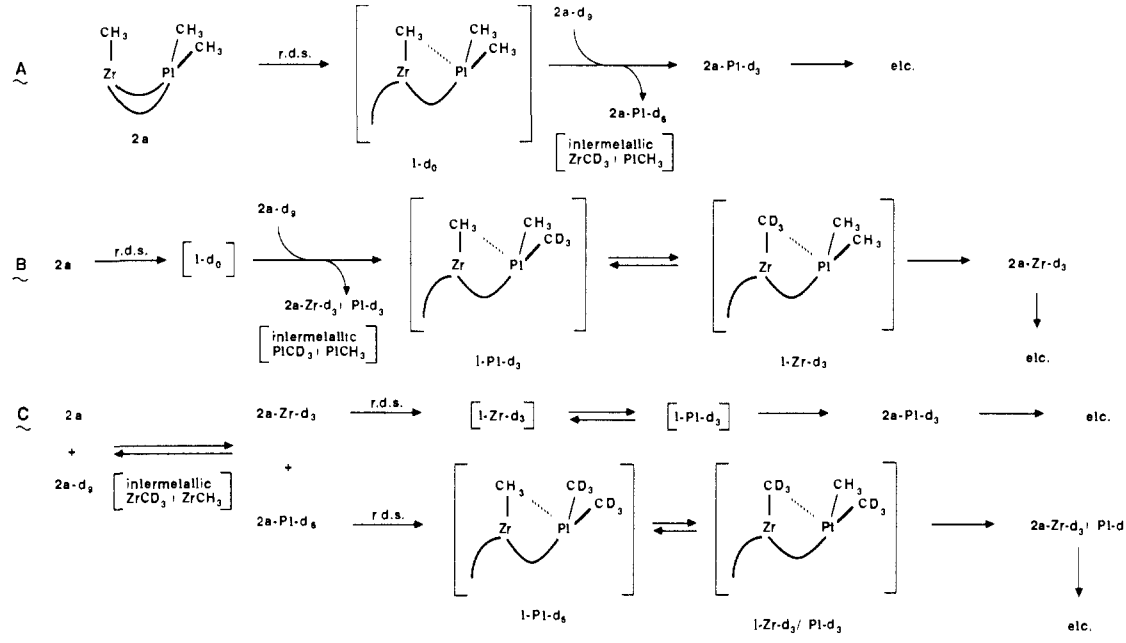

lecular bimetallic step (either Scheme I or II; the latter is illustrated).

Further Crossover/Kinetics. In order to test the possibility that bimolecular PtMe/PtMe exchanges were responsible for the scrambling, the Zr-bound Me of **2a** was replaced with an iodide. Treatment of $Cp^*ZrMe(\mu\text{-}OCH_2Ph_2P)_2PtMe_2$ (**2a**) with CH_3I afforded *cis*-$Cp^*ZrI(\mu\text{-}OCH_2Ph_2P)_2PtMe_2$ (**6**, ~69%, eq 11) as an off-white solid that contained ~10% impurities which could not be removed. Again, $^{195}Pt\{^1H\}$ NMR was used to monitor the thermolysis of **6** (δ −4692) and **6-d_6** (eq 12). Although the kinetic

$$\mathbf{2a} \xrightarrow[92\ ^\circ C,\ 10\ h]{CH_3I} \textit{cis}\text{-}Cp^*ZrI(\mu\text{-}OCH_2Ph_2P)_2PtMe_2 + C_2H_6 + \ldots \quad (11)$$

$$\mathbf{6} + \mathbf{6}\text{-}d_6 \underset{k}{\overset{2k}{\rightleftharpoons}} Cp^*ZrI(\mu\text{-}OCH_2Ph_2P)_2Pt(CH_3)(CD_3) \quad (12)$$
$$\mathbf{6}\text{-}d_3$$

investigation of the crossover to **6-d_3** was limited, the results were informative. The PtMe/PtMe exchange was roughly first order, and the rate (k = 5 (2) × 10^{-7} s^{-1}) only a factor of ~3 slower than the ZrMe/PtMe and scrambling rates of **2a**, lending credence to the possibility that the crossover of Me's in the latter is due to a similar post-rate-determining step (B in Scheme III). If phosphine dissociation is assisted (Scheme II), then substitution of Me by I should affect the rate, although an increase might be expected because iodide is a capable bridge. Note that the slow exchange in eq 12 corroborates the aforementioned elimination of possible pre-rate-determining PtMe/PtMe transfers.

In reviewing the preceding crossover experiments, it is pertinent to discuss how bimolecular exchanges of the ZrMe/PtMe or PtMe/PtMe type could take place. Recall that Scheme II contains a step where rate-determining assisted (or direct) dissociation of a phosphine sets the stage for Me/Me exchange. In both cases, the resulting Pt moiety is either a 14 e^- or weakly μ-Me coordinated square-planar species, therefore exposed for attack. In Scheme IV the exchanges are *viewed under the simplifying conditions of early conversion* by using proposed pathways (A, B, and C) of the **2a-Zr-d_3** to **2a** and **2a-Zr-d_3/Pt-d_3** transformation. Once the phosphine is lost (k_1), generating **I-Zr-d_3**, the site of unsaturation may be captured bimolecularly by a $D_3CZrCp^*(\mu\text{-}O\text{-})_2$ fragment of another **2a-Zr-d_3** molecule (k_b), representing the intermetallic, intermolecular exchange process, A. The unsaturated Pt-center of **I-Pt-d_3** may be similarly trapped ($k_{b'}$) in a bimolecular, post-rate-determining $PtCH_3/PtCD_3$ swap (B). If the phosphine reattaches (k_c) after all pertinent exchanges have occurred, the methyl redistributions in A (k_b[**2a-Zr-d_3**] ≫ k_c: rate = k_1[**2a-Zr-d_3**]) and B ($k_{b'}$[**2a-Zr-d_3**] ≫ k_{-1}: rate = $2k_1$[**2a-Zr-d_3**]) will be first order. In pathway C, it is assumed that any ZrMe/ZrMe swap is fast compared to k_1, hence the rate = $2k_1$[**2a-Zr-d_3**] at early conversion.

In principle, the rate-determining step of the intermetallic Me/Me exchange could be shifted from uni- to bimolecular (e.g., $(k_1/k_c)k_b$[**2a-Zr-d_3**]^2 at early conversion) by diminishing the concentration of **2a-Zr-d_3**. Unfortunately, the low solubility and high sensitivity of the complex have limited the concentrations (0.112–0.0102 M) amenable to study. In view of the latter possibility, consider this scenario. Assume that the initial concentration of **2a-Zr-d_3** is 0.01 M and that the rate-determining step for exchange involves the previously discussed phosphine dissociation (k_1); its rate constant is ~2 × 10^{-6} s^{-1} (~100 °C). After dissociation, a bimolecular exchange (k_b) may take place, or the phosphine may reconnect to the Pt (k_c). An approximate minimum for k_c is ~2 × 10^{-5} s^{-1}, since the phosphine-dissociated intermediate is unobserved (given that a generous 10% of the dissociated complex must be present for spectroscopic detection). Assume that for a first-order reaction the bimolecular exchange must be ~10 times faster than reformation of the Pt–P bond. The bimolecular rate constant (k_b) must therefore be ~2 × 10^{-2} M^{-1} s^{-1}, quite a reasonable value given the assumptions above.

This logic is correct, yet a problem point exists; the value for the recombination of the Pt–P linkage (k_c) is expected to be far greater than 2 × 10^{-5} s^{-1}. By using flash photolysis techniques, Dobson[44] has measured the recombination rates of the amino portion of $Ph_2P(CH_2)_2NR_2$ chelates on $(Ph_2P(CH_2)_2NR_2)Mo(CO)_4$. In general, rate constants for reformation of the Mo–N bond are in the 10^5–10^6 s^{-1} range. Rate constants for competitive phosphine capture of the coordinatively unsaturated Mo center are ~10^4 M^{-1} s^{-1}. If these recombination rates are applicable to the bridging μ-OCH_2Ph_2P ligand of **2a-Zr-d_3**, the bimolecular exchange step (k_b) must approach the diffusion limit, ~10^8–10^9 M^{-1} s^{-1}! Granted, the similarity of a mononuclear chelate to the bridge of **2a** is tenuous, but even a modest recombination rate (e.g., k_c = 10 s^{-1}) would require that k_b be ~10^4 M^{-1} s^{-1} (given the aforementioned factor of 10), a second-order rate commensurate with phosphine trapping of a coordinatively unsaturated center.

While none of the above arguments rigorously disprove mechanisms requiring bimolecular ZrMe/PtMe (A) or PtMe/PtMe (B) exchanges, they certainly suggest that such processes may be unrealistic and that the validity of the PtMe/PtMe ex-

(44) Dobson, G. R.; Bernal, I.; Reisner, G. M.; Dobson, C. B.; Mansour, S. E. *J. Am. Chem. Soc.* **1985**, *107*, 525–532.

Scheme IV

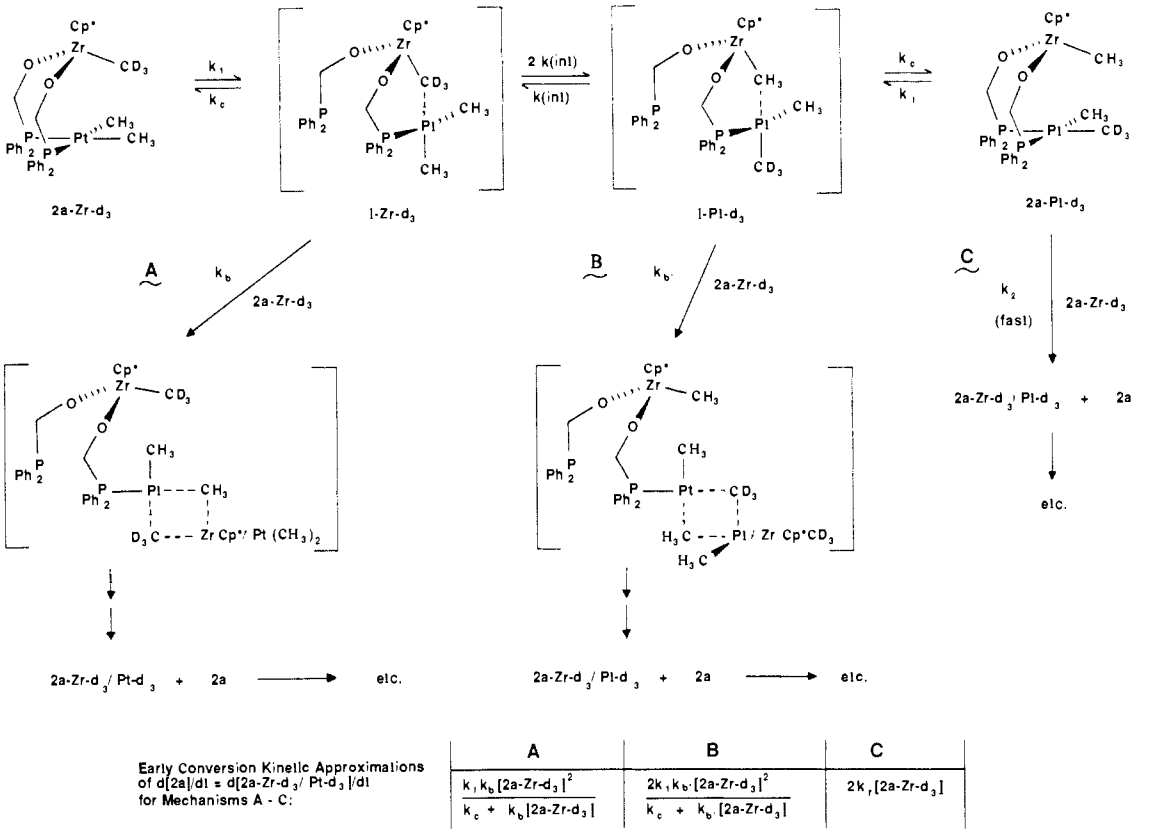

changes of **6** must also be carefully scrutinized. There remains the possibility that a fast ZrMe/ZrMe swapping occurs prior to an intra (C) or intermolecular ZrMe/PtMe exchange. Devising an experiment to test this postulation proved difficult, given the constraints of observation by NMR methods.

One perturbation considered to provide additional information was the utilization of an additional methylene unit in the bridge. When $(HOCH_2CH_2Ph_2P)_2PtMe_2$ (**1b**) and Cp^*ZrMe_3 were mixed in toluene, the evolution of methane was noted, and after 4 h *cis*-$Cp^*ZrMe(\mu\text{-}OCH_2CH_2Ph_2P)_2PtMe_2$ (**2b**) could be isolated in ~85% purity and ~72% yield (eq 13). From the *cis*-PtP

$$\mathbf{1b} + Cp^*ZrMe_3 \rightarrow \underset{\mathbf{2b}}{cis\text{-}Cp^*ZrMe(\mu\text{-}OCH_2CH_2Ph_2P)_2PtMe_2} + 2CH_4 \quad (13)$$

coupling constant (1890 Hz),[23,24] the coordination about Pt is close to that of **2a** ($J_{cis\text{-}PtP}$ = 1830 Hz). In contrast to the synthesis of **2a**, extended reaction times were unnecessary. It is conceivable that post-alcoholysis conproportionation reactions are more facile with the more open, longer chain bridge. Despite failures to further purify **2b**, parallel kinetic investigations of the complex were undertaken at 96.4 °C. The Me/Me exchange rate was again monitored via approach to equilibrium kinetics at 96.4 °C by using **2b-Zr-*d*₃**. A first-order rate (3 (1) × 10^{-5} s^{-1}) was observed, and crossover was detected via $^{195}Pt\{^1H\}$ NMR as **2b-Zr-*d*₃** gave rise to both **Pt-*d*₃** (**2b-Pt-*d*₃**, **2b-Zr-*d*₃/Pt-*d*₃**) and **Pt-*d*₆** (**2b-Pt-*d*₆**, **2b-*d*₉**) products. The apparent exchange and crossover rates of **2b** are approximately 20 times more facile than that of **2a**, perhaps an indication of a less constrained geometry. Regardless, the results portray similar mechanistic pathways for the differing bridges.

Anticipating the discovery of a swift bimolecular ZrMe/ZrMe exchange,[43] **2a** and **2b-Zr-*d*₃** were checked for crossover; kinetic monitoring of the approach to equilibrium in eq 14 at 25 °C

$$\mathbf{2a} + \mathbf{2b\text{-}Zr\text{-}}d_3 \overset{25\ ^\circ C}{\rightleftharpoons} \mathbf{2a\text{-}Zr\text{-}}d_3 + \mathbf{2b} \quad (14)$$

yielded a second-order rate constant of 4 × 10^{-4} M^{-1} s^{-1}. Extrapolating to the temperatures used to monitor the ZrMe/PtMe exchange (eq 7/9) revealed that ZrMe/ZrMe exchange would *always be faster* than the apparent bimetallic exchange, given the concentrations of the heterobimetallics used in this study.[45] For this extrapolation to be considered, one obvious assumption is necessary; the ZrMe/ZrMe transfers involving **2a** isotopomers are considered to occur at about the same rate as the crossover in eq 14. While a minor steric inhibition might be expected for the self-exchange of **2a**, it should be relatively inconsequential based on molecular models.[45] Hence, mechanism C, comprised of pre-rate-determining ZrMe/ZrMe swaps and intramolecular bimetallic Me/Me exchanges, is fully consistent with all data and arguments presented thus far.

Equimolar amounts of **2a-Zr-*d*₃** and **2b-Zr-*d*₃** were placed in solution, and the Zr–Me signals of each were monitored (the Pt–Me resonances of **2a** and **2b** overlap and cannot be evaluated) for the appropriate exchange by ^1H NMR. Both Zr–CH_3 groups grew in at the same rate, inconsistent with pathway B which would predict that the Zr methyl of **2b** would appear at ~20 times the rate of its cognate. This experiment did not eliminate the possibility that either A, C or a combination of B and C were operative. However, monitoring via $^{195}Pt\{^1H\}$ NMR revealed that signals pertaining to **2b-Pt-*d*₃**, **2b-Zr-*d*₃/Pt-*d*₃**, **2b-Pt-*d*₆**, and **2b-*d*₉** grew in 20 times faster than the corresponding **2a** isotopomers. If post-rate-determining PtMe/PtMe exchanges had occurred, a commensurate growth of the **2b** and **2a** deuterium-containing Pt isotopomers was anticipated because of the following. Although **2b** would dissociate its phosphine 20 times more often than **2a**, its coordinatively unsaturated Pt center could choose a Pt–Me from either **2a** or **2b**, effectively deuteriating both Pt centers at

(45) As a crude estimate, consider the bimolecular rate to double every 10 °C. At 84.6 °C, k(ZrMe/ZrMe) ≅ 2.5 × 10^{-2} M^{-1} s^{-1} and at 96.4 °C, k ≅ 5 × 10^{-2} M^{-1} s^{-1}. The corresponding pseudo-first-order rate constants at 0.0622 M are 1.6 × 10^{-3} and 3 × 10^{-3} s^{-1}. Thus the bimetallic ZrMe/ZrMe exchange is approximately 2000–3000 times faster than an intramolecular ZrMe/PtMe exchange. At the lowest concentration used (0.0102 M), the rate discrepancy would still be a factor of ~300–500. The bimetallic rate of the self-exchange of **2a** isotopomers is predicted to be somewhat slower based on steric arguments but not by enough to override the rate differences addressed above.

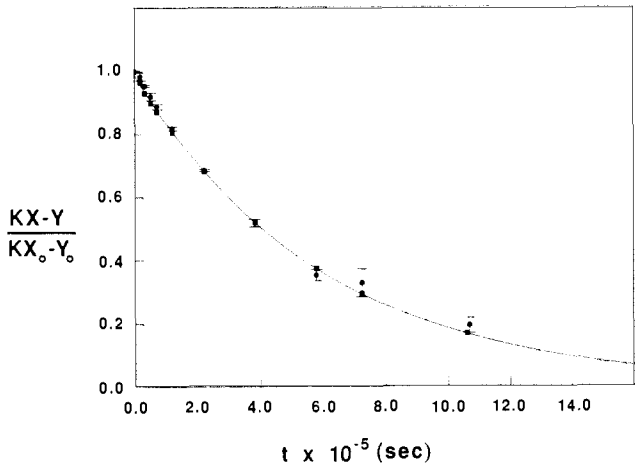

Figure 4. Fit of observed (●, 1 sd) and simulated (■, $k_1 = 5.56 \times 10^{-7}$ s^{-1}, $k_2 = 4 \times 10^{-4}$ M^{-1} s^{-1}) data corresponding to thermolysis of **2a-Zr-d_3** at 84.6 °C. The observed k_1, from a nonlinear, weighted least-squares fit, was 5.56 (1) $\times 10^{-7}$ s^{-1} (see ref 48).

the same rate! Model studies again support the contention that steric differences between the two Pt centers are insignificant. On the basis of these experiments and previous arguments regarding the value of $k_{b'}$ (Scheme IV, B), *mechanism B, with or without additional ZrMe/ZrMe scrambling, is dismissed.* In addition, any pathway utilizing transfers of $PtMe_2$ moieties may be discredited on the basis of the experiments above.[46]

Kinetics Modeling. If the most straightforward pathway for exchange and crossover consists of fast bimolecular ZrMe/ZrMe steps coupled to intramolecular ZrMe/PtMe exchange, eq 15–19

Intramolecular ZrMe/PtMe:

$$\textbf{2a-Zr-}d_3 \underset{k_{-1}}{\overset{2k_1}{\rightleftharpoons}} \textbf{2a-Pt-}d_3 \quad (15)$$

$$\textbf{2a-Pt-}d_6 \underset{k_{-1}}{\overset{2k_1}{\rightleftharpoons}} \textbf{2a-Zr-}d_3/\textbf{Pt-}d_3 \quad (16)$$

Intermolecular ZrMe/ZrMe:

$$\textbf{2a} + \textbf{2a-}d_9 \underset{k_2}{\overset{k_2}{\rightleftharpoons}} \textbf{2a-Zr-}d_3 + \textbf{2a-Pt-}d_6 \quad (17)$$

$$\textbf{2a} + \textbf{2a-Zr-}d_3/\textbf{Pt-}d_3 \underset{k_2}{\overset{k_2}{\rightleftharpoons}} \textbf{2a-Zr-}d_3 + \textbf{2a-Pt-}d_3 \quad (18)$$

$$\textbf{2a-}d_9 + \textbf{2a-Pt-}d_3 \underset{k_2}{\overset{k_2}{\rightleftharpoons}} \textbf{2a-Pt-}d_6 + \textbf{2a-Zr-}d_3/\textbf{Pt-}d_3 \quad (19)$$

should be sufficient to describe the overall kinetics. An important question remains. Are the apparent rates of bimetallic Me/Me exchange (k'_1 of eq 9 and 10) and the ^{195}Pt NMR-observed scrambling rates equivalent to the microscopic rate, k_1 of eq 15 and 16, which corresponds to the true bimetallic transfer? If the observed is different from the true exchange, ΔS^* (Figure 2) would not represent a discrete transition state and would be heavily weighted by the statistical distribution of the complex process.

In the Appendix, comparisons of the various observed and derived rate constants indicate that the former *do correspond* to k_1, given the constraints of mechanism C of Scheme III (k_2[**2a**] $\gg k_1 = k_{-1}$). In addition, Runge–Kutta numerical integration methods[32,47] corroborated the derivations and provided calculated data for comparison (Figure 4 shows observed versus calculated data for the 84.6 °C run, with $k_1 = 5.56 \times 10^{-7}$ and $k_2 = 4 \times 10^{-4}$ M^{-1} s^{-1}, see Appendix).[48] The kinetic model indicated by eqs 15–19 represents a viable pathway which adequately encompasses the observed ZrMe/PtMe exchanges and crossovers.[49]

(46) For example, attack by a pendant dissociated phosphine linkage on the Pt center of another **2a** isotopomer would engender an associative substitution. Subsequent phosphine exchanges would result in the transfer of a $PtMe_2$ fragment. Recall, however, that added PPh_3 destroys **2a** within minutes of addition.

(47) Milne, W. E. *Numerical Solutions of Differential Equations*; Wiley: New York, 1953; pp 72–73.

Conclusion

The objective of this study, the observation of Me/Me ligand exchange in a heterobimetallic containing widely disparate metal centers, has clearly been reached. A significant kinetic barrier, primarily enthalpic in origin, has been observed, yet it may not directly reflect alkyl migration if Pt–P bond weakening dominates the energetics of the transition state. Similar alkyl migrations across heterogeneous interfaces may also occur, provided thermodynamic constraints are not dominant. Processes where alkyl migrations could be critical (i.e., Fischer–Tropsch, reforming)[1-4] utilize temperatures which should facilitate interfacial alkyl transfer. The phenomenon of hydrogen spillover[18] provides an example of a similar migration. Hydrogen adsorbs onto a surface, usually a late metal, and then moves across an interface to a second surface, typically a support material inert to the direct reaction of H_2. A plausible metal-to-support migration of alkyls in heterogeneous systems can be considered analogously.

As a consequence of monitoring a statistical redistribution of Me groups between the Pt and Zr centers of Cp*ZrMe(μ-$OCH_2Ph_2P)_2PtMe_2$ (**2a**) isotopomers by using approach-to-equilibrium kinetics, the overall mechanism of heterobimetallic alkyl exchange cannot be determined with absolute certainty. Despite numerous complications, sequence C (Schemes III and IV), fast redistribution of Zr-methyls accompanied by rate-determining intramolecular ZrMe/PtMe exchange, possesses some clear advantages: (1) the bimolecular ZrMe/ZrMe transfers of **2a**/**2b-d_3** are about 10^3 faster than the ZrMe/PtMe exchange of **2a**; (2) molecular models of **2a** support the contention that intramolecular bimetallic exchange pathways are available; (3) the observed first-order kinetics pertaining to Me transfers and crossover reactions can be fully explained and substantiated by using numerical integration methods; (4) the critical bimolecular ZrMe/ZrMe exchange has ample literature precedence,[43] including observations which indicate that such transfers are facile; and (5) bimolecular (k_b) rates of the intermolecular ZrMe/PtMe exchanges required by A appear to be prohibitively fast, as previously addressed. This mechanistic investigation also reasserts[10] the importance of redistribution reactions in organometallic chemistry. All types of exchange, intra- and intermolecular and intra- and intermetallic, are manifested through the migration of an alkyl between transition metals, a relatively uncommon transformation.

Experimental Section

General Considerations. All manipulations were performed by using either glovebox, high vacuum line, or Schlenk line techniques. Hydrocarbon solvents were purified by initial distillation from purple sodium/benzophenone ketyl followed by vacuum transfer from same. Small amounts of tetraglyme (2–5 mL/1200 mL) were added to hydrocarbons to solubilize the ketyl. CH_2Cl_2 was twice distilled from P_2O_5. Benzene-d_6 was dried over activated 4-Å molecular sieves. Cp*$ZrMe_3$,[25] (COD)-$PtMe_2$,[19] [Cp*$RhCl_2]_2$,[29] $HOCH_2Ph_2P$,[20] and $HOCH_2CH_2Ph_2P$[21] were prepared via literature procedures.

NMR spectra were obtained on Varian XL-200 (^1H, ^{31}P), XL-400 (^{195}Pt, ^{13}C, $^{195}Pt\{^1H\}$ NMR kinetics), Bruker WM-300 (^1H, ^1H NMR kinetics), and JEOL FX90Q (^{31}P, ^{13}C) spectrometers. $^{195}Pt\{^1H\}$ NMR shifts are reported in ppm downfield of K_2PtCl_6 and $^{31}P\{^1H\}$ are referenced to PCl_3 at 219 ppm downfield from H_3PO_4. The T_1 relaxation

(48) The simulation of the 84.6 °C kinetics was conducted by using $k_1 = 5.56 \times 10^{-7}$ s^{-1} and $k_2 = 4.0 \times 10^{-4}$ M^{-1} s^{-1}. The latter rate constant was chosen because calculations indicate that it is approximately the lower limit of k_2. It is about 65 times less than the predicted rate of ZrMe/ZrMe exchange between **2a** and **2b-Zr-d_3** (eq 14, ref 45) at 85 °C. The pseudo-first-order (k_2[**2a** isotopomer]) rate constant is 2.5×10^{-5} s^{-1}, about 50 times greater than k_1.

(49) In principle, the Runge–Kutta numerical integration methods could be used to test mechanisms A and B. However, in order to model these pathways, six intermediate species would need to be introduced. Moreover, only the relative rates of $k_{b(b')}$ [**2a** isotopomer] and k_c, constrained in part by the value of k_1, control the inter- versus intramolecularity of reaction. Since neither is known, arbitrary values would need to be used in each pathway, rendering the models preordained. The illustrations and accompanying arguments of Scheme IV portray these mechanistic choices more effectively.

times were determined by using the inversion recovery method.[51] Infrared spectra recorded on a Mattson FT-IR instrument were used as fingerprints and are not reported. Elemental analyses were conducted by Analytische Laboratorien, West Germany. Molecular weights were determined by benzene freezing point depression.

Procedures. 1. *cis*-$PtMe_2(PPh_2CH_2OH)_2$ (1a). To a flask containing $(COD)PtMe_2$ (0.700 g, 2.10 mmol) and $HOCH_2Ph_2P$ (0.908 g, 4.20 mmol) was added 10 mL of CH_2Cl_2 at −78 °C. The solution was warmed to 25 °C, stirred for 3 h, and reduced in volume to 5 mL. Hexane (~5 mL) was added to precipitate **1a**, which was isolated by filtration and dried under vacuum (1.111 g, 81%): ^1H NMR (C_6D_6) δ 1.17 (Me, dd, 6 H, J_{PH} = 6, 8, J_{PtH} = 68 Hz), 2.50 (OH, br s, 2 H), 4.07 (CH_2, s, 4 H, $^3J_{PtH}$ = 8 Hz), 6.93 (Ph, m, 12 H), 7.48 (Ph, m, 8 H); $^{13}C\{^1H\}$ NMR (C_6D_6) δ 6.88 (Me, dd, J_{PC} = 87, 14 Hz, J_{PtC} = 598 Hz), 61.63 (CH_2, m), 126.8–133.7 (Ph); $^{31}P\{^1H\}$ NMR (C_6D_6) δ 19.02 (J_{PtP} = 1819 Hz). Anal. Calcd for $C_{28}H_{32}O_2P_2Pt$: C, 50.99; H, 4.89. Found: C, 50.96; H, 4.74.

2. *cis*-$PtMe_2(PPh_2CH_2CH_2OH)_2$ (1b). Procedure 1 was followed by using $HOCH_2CH_2Ph_2P$ (0.545 g, 2.37 mmol) and $(COD)PtMe_2$ (0.390 g, 1.16 mmol), added via a sidearm, yielding 468 mg **1b** (63%): ^1H NMR (CD_2Cl_2) δ 0.42 (Me, dd, 6 H, J_{PH} = 6, 8 Hz, J_{PtH} = 68 Hz), 2.40 (PCH_2, 'dt', 4 H), 3.07 (OH, t, 2 H), 3.75 (OCH_2, m, 4 H), 7.20–7.44 (Ph, m, 20 H); $^{31}P\{^1H\}$ NMR (CD_2Cl_2) δ 9.32 (J_{PtP} = 1748 Hz). Anal. Calcd for $C_{30}H_{36}O_2P_2Pt$: C, 52.55; H, 5.29. Found: C, 52.44; H, 5.28.

3. *cis*-$Cp^*ZrMe(\mu\text{-}OCH_2Ph_2P)_2PtMe_2$ (2a). To a flask containing **1a** (0.454 g, 0.69 mmol) and Cp^*ZrMe_3 (0.189 g, 0.70 mmol) was transferred 25 mL of toluene at −196 °C. The mixture was warmed to −78 °C and stirred for 10 min as gas evolution was noted. Upon further warming to 25 °C, vigorous gas evolution continued. The mixture was stirred for another 48 h, and the toluene was removed until a 1-mL solution remained. Hexane (10 mL) was added to give an off-white precipitate which was filtered, washed with hexane, and dried under vacuum (564 mg, 91%): ^1H NMR (C_6D_6) δ 0.62 (ZrMe, s, 3 H), 1.22 ($PtMe_2$, dd, 6 H, J_{PH} = 6, 8 Hz, J_{PtH} = 68 Hz), 2.07 (Cp^*, s, 15 H), 4.69 (CH_2, m, 4 H), 6.90 (Ph, m, 12 H), 7.47 (Ph, m, 8 H); $^{13}C\{^1H\}$ NMR (C_6D_6) δ 8.99 ($PtMe_2$, dd, J_{PC}(trans) = 99, J_{PC}(cis) = 8 Hz, J_{PtC} = 616 Hz), 10.31 ($C_5(CH_3)_5$), 29.24 (ZrMe), 68.89 (CH_2, m, AMXX'), approximate couplings: $^2J_{PtC}$ = 1.6, $^3J_{PC}$ = 2.5, J_{CP} = 30, $^2J_{PP}$ = 6, J_{PtP} = 1830 Hz), 118.48 (C_5Me_5), 129–136 (Ph); $^{31}P\{^1H\}$ (C_6D_6) δ 18.31 (J_{PtP} = 1830 Hz); $^{195}Pt\{^1H\}$ NMR (C_6D_6) δ −4690 (t, J_{PtP} = 1830 Hz). Anal. Calcd for $C_{39}H_{48}O_2P_2ZrPt$: C, 52.22; H, 5.39. Found: C, 52.04; H, 5.35. M_r found 816, calcd 897.

4. *cis*-$Cp^*ZrMe(\mu\text{-}OCH_2CH_2Ph_2P)_2PtMe_2$ (2b). To a flask containing **1b** (270 mg, 0.39 mmol) and Cp^*ZrMe_3 (106 mg, 0.39 mmol) was transferred 10 mL of toluene at −196 °C. The mixture was warmed to −78 °C, and gas evolved. After slowly warming to 25 °C (2–3 h) and stirring for an additional 2 h, the toluene was removed until ~3 mL remained. Hexane (15 mL) was added to precipitate a white solid, which was isolated by filtration, washed with hexane, and dried in a vacuum (260 mg, 72%, purity variable (85–90%), see below): ^1H NMR (C_6D_6) δ 0.43 (ZrMe, s, 3 H), 1.18 ($PtMe_2$, dd, 6 H, J_{PH} = 6, 8, J_{PtH} = 68 Hz), 2.06 (Cp^*, s, 15 H), 4.04 (CH_2P, m, 4 H), 4.35 (OCH_2, m, 4 H), 7.01 (Ph, m, 12 H), 7.50 (Ph, m, 8 H); $^{13}C\{^1H\}$ (C_6D_6) δ 6.14 ($PtMe_2$, dd, J_{PC}(cis) = 9, J_{PC}(trans) = 100, J_{PtC} = 607 Hz), 10.77 ($C_5(CH_3)_5$), 26.50 (ZrMe), 31.10 (PCH_2, AMXX'), 65.37 (OCH_2, t, J_{PC} = 6.5 Hz), 118.44 (C_5Me_5), 127.5–138.5 (Ph); $^{31}P\{^1H\}$ (CD_2Cl_2) δ 10.66 (J_{PtP} = 1890); $^{195}Pt\{^1H\}$ (C_6D_6) δ −4618 (t, J_{PtP} = 1890); M_r found 900, calcd 925. By $^{31}P\{^1H\}$ NMR, two impurities were noted; one (5–10%) identified as **1b** and another of unknown structure (5–10%, no J_{PtP}). By ^1H NMR, integration of the Cp* region indicated the presence of varying amounts (5–15%) of unidentifiable impurities.

5. $Cp^*RhCl_2(PPh_2CH_2OH)$ (3). To a flask containing $[Cp^*RhCl_2]_2$ (1.523 g, 2.464 mmol) and $HOCH_2Ph_2P$ (1.065 g, 4.931 mmol) was distilled 50 mL of CH_2Cl_2 at −78 °C. The solution was allowed to warm to 25 °C and was stirred for 5 h. Upon removal of ~45 mL of CH_2Cl_2 and addition of 30 mL of hexane an orange precipitate formed. The solid was collected by filtration and washed once with 10 mL of hexane to yield 2.52 g of **3** (97%): ^1H NMR ($CDCl_3$) δ 1.42 (Cp^*, d, 15 H, J_{RhH} = 4 Hz), 3.85 (OH, td, 1 H, J_{PH} = 3 Hz, J_{HH} = 7 Hz), 4.75 (CH_2, d, 2 H, J_{HH} = 7 Hz), 7.34 (Ph, m, 6 H), 7.68 (Ph, m, 4 H); $^{31}P\{^1H\}$ NMR ($CDCl_3$) δ 22.45 (d, J_{RhP} = 144 Hz).

6. $Cp^*ZrCl_2(\mu\text{-}OCH_2Ph_2P)RhMe_2Cp^*$ (4). To a solution of Cp^*ZrMe_3 (775 mg, 2.86 mmol) in 12 mL of toluene at 25 °C was added **3** (1.500 g, 2.86 mmol) over a 20-min period. During 6 days of stirring, a light yellow precipitate formed. The toluene was removed and replaced with pentane. The product was collected by filtration and washed twice (5 mL) with pentane, yielding 1.74 g of light yellow crystalline **4** (78%): ^1H NMR (C_6D_6) δ 0.34 ($RhMe_2$, dd, 6 H, J = 3, 4 Hz), 1.43 ($RhCp^*$, d, 15 H, J_{RhH} = 2 Hz), 1.73 ($ZrCp^*$, s, 15 H), 5.15 (CH_2, d, 2 H, J = 3 Hz), 7.24 (Ph, m, 6 H), 7.65 (Ph, m, 4 H); $^{31}P\{^1H\}$ NMR (C_6D_6) δ 50.65 (J_{RhP} = 168 Hz). Anal. Calcd for $C_{35}H_{48}OPCl_2ZrRh$: C, 53.84; H, 6.20; Cl, 9.08. Found: C, 53.71; H, 6.13; Cl, 8.98.

7. $Cp^*ZrMe_2(\mu\text{-}OCH_2Ph_2P)RhMe_2Cp^*$ (5). To a flask containing **4** (1.200 g, 1.539 mmol) and 30 mL of Et_2O at −78 °C was added 5.0 mL (3.2 mmol) of CH_3MgBr (0.64 M in Et_2O). After being stirred at −78 °C for 2–3 h, the reaction mixture was warmed to 25 °C and stirred for 2 days. The diethyl ether was removed and replaced with 20 mL of benzene. Filtration and washing of the precipitated salt gave a red solution. The benzene was replaced with pentane, and the resulting yellow microcrystals were filtered and washed (3 × 2 mL) with pentane to yield **5** (910 mg, 80%): ^1H NMR (C_6D_6) δ −0.24 ($ZrMe_2$, s, 6 H), 0.36 ($RhMe_2$, dd, 6 H, J = 3, 5 Hz), 1.46 ($RhCp^*$, d, 15 H, J = 2 Hz), 1.70 ($ZrCp^*$, s, 15 H), 5.10 (CH_2, d, 2 H, J = 2 Hz), 7.18 (Ph, m, 6 H), 7.69 (Ph, m, 4 H); $^{31}P\{^1H\}$ NMR (CD_2Cl_2) δ 50.45 (J_{RhP} = 168 Hz). Anal. Calcd for $C_{37}H_{48}D_6OPZrRh$: C, 59.57; H, 7.30. Found: C, 59.28; H, 7.17.

8. $Cp^*ZrI(\mu\text{-}OCH_2Ph_2P)_2PtMe_2$ (6). To a tube sealed to a joint attached to a needle valve adapter were added **2a** (204 mg, 0.239 mmol) and 10 mL of benzene. Methyl iodide (32.6 mg, 0.23 mmol), measured via a gas bulb, was condensed into the tube at −196 °C. The tube was then sealed with a torch and heated to 92 °C for 10 h. The tube was cracked, and the contents were transferred to a flask where the volume was reduced to ~2 mL. Upon addition of 10 mL of hexane, a white solid precipitated. The solid was triturated with hexane, filtered, washed twice with hexane, and dried in vacuo (162 mg, 69%, purity variable (~90%), see below): ^1H NMR (C_6D_6) δ 1.15 (PtMe, dd, 6 H, J_{PH} = 6, 8 Hz, J_{PtH} = 69 Hz), 2.15 (Cp^*, s, 15 H), 4.64 (CHH, dt, 2 H, $^2J_{HH}$ = 12 Hz, J_{PH} = 8 Hz), 4.94 (CHH, dt, 2 H, $^2J_{HH}$ = 12 Hz, J_{PH} = 6 Hz), 6.7–7.6 (Ph, m, 20 H); $^{13}C\{^1H\}$ (C_6D_6) δ 10.29 ($PtMe_2$, dd, J_{PC} = 8, 100 Hz, J_{PtC} = 621 Hz), 12.59 ($C_5(CH_3)_5$), 71.11 (CH_2, AMXX'), 124.25 (C_5Me_5), 128.01 (Ph, d, J_{PC} = 25 Hz), 129.42 (Ph, d, J_{PC} = 38 Hz), 133.16 (Ph, m), 135.04 (Ph, m); $^{31}P\{^1H\}$ NMR (C_6D_6) δ 16.45 (J_{PtP} = 1865 Hz); $^{195}Pt\{^1H\}$ (C_6D_6) δ −4692 (t, J_{PtP} = 1865 Hz); M_r found 978, calcd 1009. By investigating the Cp* region of the ^1H NMR spectrum, about 10% Cp*-containing impurities are evident. The $^{31}P\{^1H\}$ spectrum shows an impurity (~10%) at about δ 32. These were not identified.

General Kinetics. Solutions for kinetics were prepared in 5-mL volumetric flasks by using C_6D_6, transferred to oven-dried, 5-mm NMR tubes, freeze–pump–thaw degassed four cycles, and flame-sealed under vacuum. With solutions less than 0.0102 M, degradation of **2a** isotopomer was introduced during the latter process, presumably due to trace amounts of H_2O released upon sealing. For example, the rate constant for the approach-to-equilibrium by a 0.0102 M solution of **2a-Zr-*d*$_3$** was 7.1 (**4**) × 10^{-7} s^{-1}; while this run was clearly in a first-order regime (see Table I), some decomposition had occurred, resulting in inaccurate NMR integrations. Correcting for impurities brought the rate constant to near (~ 1.4 × 10^{-6} s^{-1}) the expected value but with much uncertainty. The data is nonetheless considered to clearly support the first-order process, thereby setting its lower limit at [**2a-Zr-*d*$_3$**] = 0.01 M.

The tubes were heated in a polyethylene glycol bath (average MW = 570–630) with a Polyscience Model 73 Immersion Circulator and were cooled quickly to ~20 °C in cold water after being removed from the bath. The bath temperatures were stable to ±0.2 °C as determined by an NBS-calibrated thermometer.

Alkyl Exchange by ^1H NMR. Exchange rates used in the determination of activation parameters were the result of data averaged over three tubes run simultaneously. A selected number of tubes contained an internal standard. The 75.6, 84.6, and 96.4 °C reactions were monitored to 2.5–3.0 half-lives and the 111.8 and 122.4 °C runs to 2.0 half-lives. For the higher temperature runs, it was impossible to obtain reliable data at longer reaction times because peaks due to decomposition interfered with resonances of the **2a** isotopomer being observed. As delineated in the appendix, the Pt–Me and Zr–Me resonances were both utilized in the determination of the bimetallic Me/Me exchange rate. The **2a** degradation rates (at 111.8 and 122.4 °C), obtained by monitoring the disappearance of unlabeled **2a** relative to an internal standard, could be used to correct the exchange rates at >2.0 half-lives. The corrected data continued to display first-order kinetics, thus the degradation products did not interfere with the alkyl transfer. Changes in pulse delay did not affect the relative integrations (delays of ca. 4 × T_1 were used). Rates and uncertainties of bimetallic exchange were obtained by using nonlinear least-squares fitting to appropriate exponential forms of the rate expressions in the Appendix.[52] Activation parameters were

(50) Frost, A. A.; Pearson, R. G. *Kinetics and Mechanism*; John Wiley and Sons: New York, 1961; pp 173–177.

(51) Levy, G. C.; Peat, E. R. *J. Magn. Reson.* **1975**, *18*, 500–521.

(52) Bevington, P. R. *Data Reduction and Error Analysis for the Physical Sciences*; McGraw-Hill: New York, 1969; Chapter 11.

obtained by using three methods: (1) unweighted linear least squares gave $\Delta H^{\ddagger} = 30.0 \pm 1.7$ kcal/mol and $\Delta S^{\ddagger} = -4 \pm 5$ eu; (2) weighted, linear least squares gave $\Delta H^{\ddagger} = 29.6 \pm 1.0$ kcal/mol and $\Delta S^{\ddagger} = -5 \pm 3$ eu by using weights of $1/\sigma^2$ where σ corresponds to $\Delta \ln \{k/T\}$, the absolute uncertainty in $\ln \{k/T\}$; and (3) weighted, nonlinear least squares gave $\Delta H^{\ddagger}$ 29.3 ± 1.3 kcal/mol and $\Delta S^{\ddagger} = -6 \pm 2$ eu by using weights of $1/\sigma^2$ where σ in this case corresponds to Δk, the absolute uncertainty in each rate constant. The methyl transfer of **2a-Pt-d_6** and heterobimetallic exchanges of the **2b** isotopomers were obtained by using two tubes run simultaneously. A temperature of 96.4 °C proved most convenient in terms of fast data acquisition with little decomposition. Data for the fast ZrMe/ZrMe exchange of **2a-Zr-d_3/2b** (eq 14) was obtained at 25 °C in a fashion similar to the above.

Crossover by ^{195}Pt {^{1}H} NMR. All reactions monitored by ^{195}Pt{^{1}H} NMR were conducted at 96.4 °C. The kinetic treatments, as described in the Appendix, were the result of averaged data from two NMR tubes, simultaneously run. Monitoring by ^{195}Pt{^{1}H} NMR was accomplished through integration of resonances from the various $PtMe_2$ (d_0, d_3, d_6) isotopomers. Pulse delays of $>10 \times T_1$ were used. Reactions were examined for 1.5–2.0 half-lives in order to minimize machine time and expense.

Acknowledgment. Support from the donors of the Petroleum Research Fund, administered by the American Chemical Society, and Cornell University is gratefully acknowledged. We thank the ARCO Foundation (S.M.B., G.S.F.) and the Shell Companies Foundation (S.M.B.) for fellowships and the NIH and NSF Instrumentation Programs for support of the Cornell NMR Facility. Prof. Barry K. Carpenter is acknowledged for helpful discussions.

Appendix

Assumptions:

1. Intermolecular ZrMe/ZrMe exchange and intramolecular ZrMe/PtMe exchange (Scheme III, C) are the most probable events which lead to the observed methyl transfers and crossover.
2. $k_1 = k_{-1}$.
3. k_2[**2a** isotopomer] $\gg k_1$.

For simplicity: [**2a-Zr-d_3**] = A; [**2a-Pt-d_3**] = B; [**2a**] = C; [**2a-Zr-d_3/Pt-d_3**] = D; [**2a-Pt-d_6**] = E; [**2a-d_9**] = F.

Restating eq 15–19:

Intramolecular ZrMe/PtMe

$$A \underset{k_1}{\overset{2k_1}{\rightleftharpoons}} B \qquad (15)$$

$$D \underset{2k_1}{\overset{k_1}{\rightleftharpoons}} E \qquad (16)$$

Intermolecular ZrMe/ZrMe

$$C + F \underset{k_2}{\overset{k_2}{\rightleftharpoons}} A + E \qquad (17)$$

$$C + D \underset{k_2}{\overset{k_2}{\rightleftharpoons}} A + B \qquad (18)$$

$$B + F \underset{k_2}{\overset{k_2}{\rightleftharpoons}} D + E \qquad (19)$$

$$\frac{dA}{dt} = k_1(B - 2A) + k_2(CF - AE + CD - AB)$$

$$\frac{dB}{dt} = k_1(2A - B) + k_2(CD - AB + ED - FB)$$

$$\frac{dC}{dt} = k_2(AB - CD + AE - CF)$$

$$\frac{dD}{dt} = k_1(2E - D) + k_2(AB - CD + FB - ED)$$

$$\frac{dE}{dt} = k_1(D - 2E) + k_2(CF - AE + FB - ED)$$

$$\frac{dF}{dt} = k_2(AE - CF + ED - FB)$$

Given: for an approach-to-equilibrium ($K = k_f/k_r$)

$$X \underset{k_r}{\overset{k_f}{\rightleftharpoons}} Y, \qquad \ln \{(KX - Y)/(KX_0 - Y_0)\} = -(k_f + k_r)t \qquad (20)$$

Case I: For the ^{1}H NMR monitoring of the intermetallic exchange via **2a-Zr-d_3** (A), the observed rate constant (k'_1 below, eq 9) is equivalent to k_1, the rate of Me transfer in eq 15.

$$[Zr\text{–}CD_3] \underset{k'_1}{\overset{2k'_1}{\rightleftharpoons}} [Pt\text{–}CD_3] \qquad (k'_1 = k'_{-1})$$

Define $(d[Zr\text{–}CH_3])/dt$ as the growth of $Zr\text{–}CH_3$ groups equivalent to $(d[Pt\text{–}CD_3])/dt$, the growth of $Pt\text{–}CD_3$ groups.

$$\frac{d[Zr\text{–}CH_3]}{dt} = \frac{dB}{dt} + \frac{dE}{dt} + \frac{dC}{dt} = 2k_1(A - E) - k_1(B - D) =$$

$$\frac{d[Pt\text{–}CD_3]}{dt} = \frac{dB}{dt} + \frac{dD}{dt} + \frac{2dE}{dt} + \frac{2dF}{dt}$$

and $$\frac{dC}{dt} = \frac{dD}{dt} + \frac{dE}{dt} + \frac{2dF}{dt}$$

Both $(d[Zr\text{–}CH_3])/dt$ and $(d[Pt\text{–}CD_3])/dt$ are of the appropriate form, thus

$$X = A - E = [Zr\text{–}CD_3]$$

$$Y = B - D = [Pt\text{–}CD_3]$$

$$K = 2 \text{ and } \ln [(2(A - E) - (B - D))/2A_0] = -3k_1t$$

Since ^{1}H NMR is used to monitor the reaction, Y is directly proportional to the integral amount of $ZrCH_3$ groups. Likewise, X is directly proportional to the integral amount of ($PtCH_3$ – $ZrCH_3$) groups divided by 2, because the Pt center has twice the number of methyls as Zr and $K = 2$ (i.e., $2k'_1/k'_1$). Given the proportionality constant ζ

$$Y = \zeta(C + B + E)$$

$$X = \frac{\zeta[(2A + 2C + B + D) - (C + B + E)]}{2} = \frac{\zeta(2A + C + D - E)}{2}$$

Substituting into eq 20

$$\ln \left[\frac{\zeta\{K(2A + C + D - E)/2 - (C + B + E)\}}{\zeta\{K(2A_0 + C_0 + D_0 - E_0)/2 - (C_0 + B_0 + E_0)\}} \right] = -3k'_1t$$

$$\ln [(2(A - E) - (B - D))/2A_0] = -3k'_1t$$

$$\therefore k_1 = k'_1$$

This derivation was checked by using simulated data from Runge–Kutta numerical integration runs. Figure 4 illustrates fits of calculated and observed data (84.6 °C)[48] to the exponential form of eq 20.

Case II: For the ^{1}H NMR monitoring of the intermetallic exchange via **2a-Pt-d_6** (E), the observed rate constant (k'_1 below, eq 10) is equivalent to k_1, the rate of Me transfer in eq 16.

$$[Zr\text{–}CH_3] \underset{k'_1}{\overset{2k'_1}{\rightleftharpoons}} [Pt\text{–}CH_3] \qquad (k'_1 = k'_{-1})$$

As in case I, but noting that the statistical distribution of CD_3 groups has reversed

$$\frac{d[Zr\text{–}CD_3]}{dt} = \frac{dA}{dt} + \frac{dD}{dt} + \frac{dF}{dt} = 2k_1(E - A) - k_1(D - B) =$$

$$\frac{d[Pt\text{–}CH_3]}{dt} = \frac{2dA}{dt} + \frac{dB}{dt} + \frac{2dC}{dt} + \frac{dD}{dt}$$

and $$\frac{dF}{dt} = \frac{dA}{dt} + \frac{dB}{dt} + \frac{2dC}{dt}$$

$$X = E - A = [Zr\text{–}CH_3]$$

$$Y = D - B = [Pt\text{–}CH_3]$$

$$K = 2 \text{ and } \ln[(2(E - A) - (D - B))/2A_0] = -3k_1t$$

Since ^1H NMR is used to monitor the reaction, X is directly proportional to the integral amount of $ZrCH_3$ groups. Likewise, Y is directly proportional to the integral amount of $PtCH_3$ groups, and K is again $2k'_1/k'_1 = 2$.

$$X = \zeta(B + C + E)$$

$$Y = \zeta(2A + 2C + B + D)$$

Substituting into eq 20:

$$\ln\left[\frac{\zeta\{K(B + C + E) - (2A + B + 2C + D)\}}{\zeta\{K(B_0 + C_0 + E_0) - (2A_0 + B_0 + 2C_0 + D_0)\}}\right] = -3k'_1t$$

$$\ln\left[(2(E - A) - (D - 2B))/2A_0\right] = -3k'_1t$$

$$\therefore k_1 = k'_1$$

This case was also checked via Runge–Kutta numerical integration methods.

Case III: For the ^{195}Pt NMR monitoring of the intermetallic exchange via **2a** (C) and **2a-d_9** (F, Figure 3), the observed rate constant is equivalent to k_1, the rate of Me transfer in eq 15 and 16.

The crossover was modeled by recognizing that the integrals of **Pt-d_0**, **Pt-d_3**, and **Pt-d_6** species are proportional to [**Pt-d_0**] (A + C), [**Pt-d_3**] (B + D) and [**Pt-d_6**] (E + F), respectively. Since $[\textbf{Pt-}d_0]_0 = C_0 = [\textbf{Pt-}d_6]_0 = F_0$, $k'_1 = k'_{-1}$. With use of the following ^{195}Pt NMR signal equilibrium

$$[\textbf{Pt-}d_0] \underset{k'_{-1}}{\overset{2k'_1}{\rightleftharpoons}} [\textbf{Pt-}d_3] \underset{2k'_1}{\overset{k'_{-1}}{\rightleftharpoons}} [\textbf{Pt-}d_6]$$

By monitoring the growth of **Pt-d_3**, eq 20 may be used

$$\frac{d[\textbf{Pt-}d_3]}{dt} = 2k'_1([\textbf{Pt-}d_0] + [\textbf{Pt-}d_6]) - 2k'_{-1}[\textbf{Pt-}d_3] = 2k'_1(A + C + E + F) - 2k'_{-1}(B + D)$$

$$X = (A + C + E + F)$$

$$Y = (B + D)$$

$$\ln\frac{K(A + C + E + F) - (B + D)}{K(A_0 + C_0 + E_0 + F_0) - (B_0 + D_0)} = -4k'_1t$$

Since $K = 1$

$$\ln\frac{(A + C + E + F) - (B + D)}{(C_0 + F_0)} = -4k'_1t$$

Alternatively

$$\frac{d[\textbf{Pt-}d_3]}{dt} = \frac{d(B + D)}{dt} = 2k_1(A + E) - k_1(B + D) = k_1(2A + 2E) - k_1(B + D)$$

Because of eq 17, the following equilibration occurs quickly, given k_2[**2a** isotopomer] $\gg k_1$: C = F = A = E. Thus

$$\frac{d[B + D]}{dt} = k_1(A + C + E + F) - k_1(B + D)$$

$$\therefore 2k'_1 = k_1$$

In essence, the $^{195}Pt\{^1H\}$ NMR method monitors a combination of the parallel paths to equilibrium given by eq 15 and 16. This method was checked via Runge–Kutta numerical integration methods.

Case IV: For the ^{195}Pt NMR monitoring of the intermetallic exchange via **2a-Pt-d_6** (E), paralleling the ^1H NMR experiments delineated in case II, the observed rate constant is *not* equivalent to k_1, the rate of Me transfer in eq 15 and 16.

The NMR equilibrium in case III also applies here, but since the route to **Pt-d_0** from **Pt-d_6** (E) involves two slow steps, the method of using this convenient (in some instances) but false equilibrium fails. Rigorous treatment of the equilibrium above as two consecutive first-order reactions[50] in combination with Runge–Kutta simulations supported this contention. The desired rate could be obtained only by looking at a simplified model—one ignoring the growth of **Pt-d_0**. At abbreviated reaction times ($< t_{1/2}$) the observed rate is approximately k_1 according to

$$-\frac{d[\textbf{Pt-}d_6]}{dt} \cong \frac{d[\textbf{Pt-}d_3]}{dt} \cong 2k_1[\textbf{Pt-}d_6] - k_1[\textbf{Pt-}d_3]$$

Again, Runge–Kutta simulations corroborated this method and indicated that substantial deviations occur at $t > t_{1/2}$. Initial rate kinetics[50] are preferred in these situations (i.e., $-d[\textbf{Pt-}d_6]/dt \cong 2k_1[\textbf{Pt-}d_6]$ at <10% conversion of **Pt-d_6**), but in this case the early conversion data was unsatisfactory due to the $^{195}Pt\{^1H\}$ NMR S/N difficulties.

Registry No. 1a, 113646-80-3; **1b**, 113646-81-4; **2a**, 113646-88-1; **2a-Zr-d_3**, 113646-89-2; **2a-Pt-d_3**, 113646-85-8; **2b**, 113646-87-0; **3**, 113646-82-5; **4**, 113646-83-6; **5**, 113646-84-7; **5-Rh-d_6**, 113646-79-0; 6, 113646-86-9; $(COD)PtMe_2$, 12266-92-1; $HOCH_2Ph_2P$, 5958-44-1; $HOCH_2CH_2Ph_2P$, 2360-04-5; Cp^*ZrMe_3, 81476-64-4; $[Cp^*RhCl_2]_2$, 12354-85-7.